Delft University of Technology
Faculty of Marine, Mechanical and Material Technology
Department of Mechanical Technology - Master - Offshore and Dredging Engineering

Master's Thesis

Improvement of on board wave height measurement

February 12, 2015

Author:
M. (Marius) Sinke

Committee:
ir. Pieter Demeersseman
dr. Elise Blondel- Couprie
Prof. dir. ir. R.H.M Huijsmans
ir. Joost den Haan

Abstract

To prepare and conduct offshore operations in safe environment, it is important to possess an accurate sea state forecast. In this thesis it is assessed whether it is possible to estimate the real time sea state at a vessel, without using any instruments deployed in the water. As a matter of fact, in-situ measurements are not always possible, for example during pipeline installation, the vessel sails a few kilometres a day, therefore the options are restricted to methods which do not include in-situ instruments. To test and validate the methods developed in this thesis real time measurements were performed on the Audacia, a pipeline installation vessel belonging to Allseas, one of the world leaders in pipeline installation. The Audacia was laying pipe nearby the coast of Australia, close to wave buoy in the Julimar Field.

Methods to extract wave field information from conventional nautical radars have been developed. It is possible to estimate a directional wave spectrum by using a temporal sequence of radar images, and following, statistical data representative of the sea state, such as the significant wave height and wave direction. However there is no unique relation between the radar images and the amount of energy in the directional wave spectrum, which result in an inaccurate significant wave height. In order to improve the directional wave spectrum estimations given by the X-Band radar used on board of the Audacia (Wavex from Miros), the possibility of using an extra measuring instrument to calibrate the energy is investigated. Two measuring devices are considered.

- A down looking radar, recently installed below the helideck of the Audacia, measuring the single point surface elevation in vicinity of the vessel. (Radac WaveGuide)
- The MRU sensors, which measure the wave induced vessel motions. (Ixsea Octans)

It is investigated whether combining the data measured by one or the other device to the X-band radar data result in an improvement of the radar estimated directional wave spectrum, and which combination gives the best results.

Method 1: Use the down looking radar measurements. The one dimensional wave spectrum given by Radac is combined with the directional wave spectrum given by Wavex. Since the Radac measurement are performed close to the vessel, the water surface is disturbed. In order to use the Radac to improve the estimated wave spectrum these disturbance have to be taken into account.
It is possible to determine a frequency dependent ratio between the amount of energy in each frequency band of the different instruments. This frequency dependent ratio is used to correct the estimated amount of energy at each frequency of the directional wave spectrum.

Method 2: Use the vessel motion measurements. In this method the measured wave induced vessel motions measured by the MRU are combined with the directional wave spectrum given by Wavex. To be able to calibrate the amount of energy in the directional wave spectrum , the radar wave spectrum has to be converted into vessel motions spectra.

Since the responses are assumed to have a linear relation with the incident wave, the ratio between the measured energy and the expected energy in the responses can be used to correct the energy estimation in the directional wave spectrum in a linear way.

After correcting the estimated directional wave spectrum with the two methods described above, the significant wave height was calculated and compared to the significant wave height given by the wave buoy in the Julimar Field. The significant wave height based on method one has a strong correlation to the significant wave height measured by the wave buoy in the Julimar Field. Method two showed that the significant wave height obtained by combining the wave field information from the nautical radar with the measured vessel motions has a less strong correlation to the significant wave height measured by the wave buoy. However, the wave spectrum given by the X-Band radar can be significantly improved in the frequency band in which the vessel responds to incident waves.

Preface

This thesis is the final work for my Master of Science study of Offshore and Dredging Engineering at the Delft University of Technology. In this thesis it is investigated whether it is possible to improve the current on board wave spectrum estimation by using an extra sensor.

I would like to use this opportunity to express my gratitude towards all the persons that provided support during my thesis, especially my thesis committee members from the university and Allseas. I would like to thank Pieter Demeerseman and Elise Blondel for their comments and suggestions.

Finally, I would like to thank my family for their interest and my lovely girlfriend Mariëlle for her great support and effort.

Contents

Chapter 1

Nomenclature

1.1 Abbreviations

ω	frequency $[rad/s]$	
θ	wave direction	$[rad]$
θ_m	mean wave direction	$[rad]$
H_{m0}, H_s	significant wave height	$[m]$
T_p	peak period	$[s]$
λ	shape parameter	
s	spreading parameter	
ϕ_{mn}	motion spectrum in direction m due to motion n	
$S(\omega, \theta)$	Directional wave spectrum	$[m^2/rad/s]$
$S(\omega)$	Wave frequency spectrum	$[m^2/rad/s]$
Rao	Response Amplitude Operator	[m/m], [rad/m]
l_{pp}	length perpendicular	[m]
I	Moment of inertia	$[kg\,m^2]$

1.2 Conventions

Vessel motion

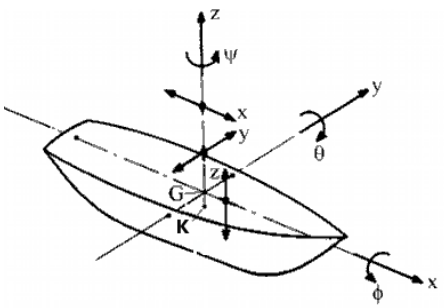

Figure 1.1: Definition of ship motion in six degrees of freedom [6]

Indication Number	symbol	Mode of motion
1	x	surge
2	y	sway
3	z	heave
4	ϕ	roll
5	θ	pitch
6	ψ	yaw

Table 1.1: Mode of motion numbered

Wave direction

In the thesis report many times is referred to wave directions, the used definition is depicted in figure 1.2.

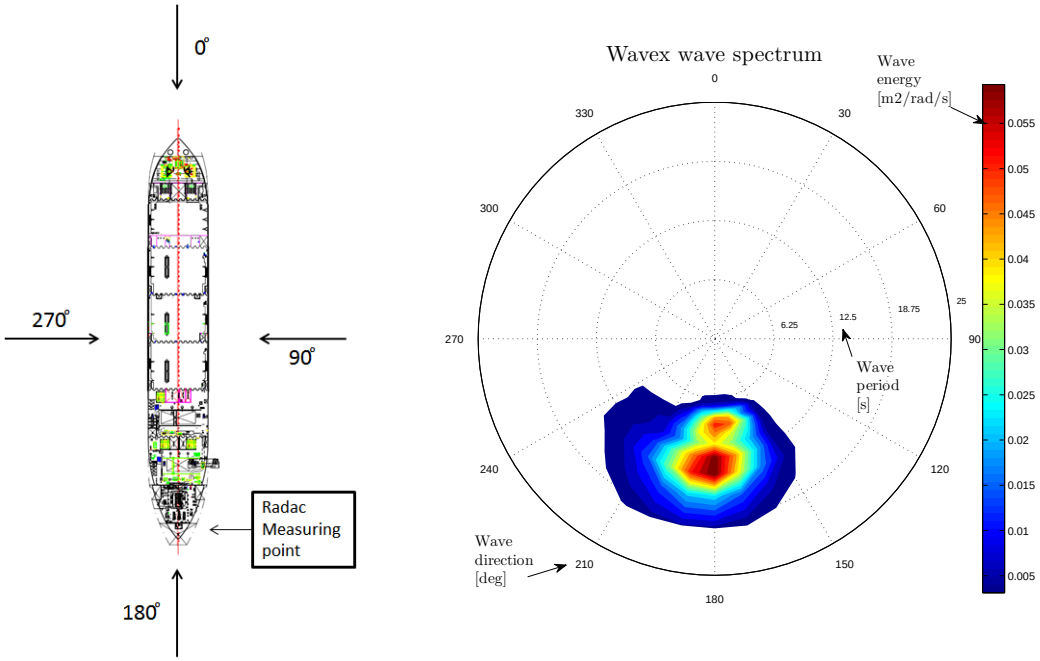

(a) Wave direction convention (b) Radar based directional wave spectrum estimation

Figure 1.2: Wave direction convention and polar plot explanation

Chapter 2

Introduction

In order to meet the growing demand of energy, the search for hydrocarbons has been expanded to desolate and hazardous places, such as the rough deep waters of the ocean. Over one third of the world's oil and gas supply is currently obtained from offshore production fields [10].

Allseas

Founded in 1985, the Swiss-based Allseas group S.A. has grown to a global leader in the offshore pipelay and subsea construction industry, and is specialised in offshore pipeline construction. Allseas main activity, before the arrival of Pioneering Spirit, was the pipe line installation. With the arrival of the new built vessel Pioneering Spirit, a multi-purpose vessel for platform installation and decommissioning, heavy lift operations will also become an important part of the Allseas core business.

2.1 Thesis background

During offshore operations, such as pipelaying or platform installation/removal, ship motions, as well as the relative motions between the ship and the pipe or the platform, are of major interest.
The larger the relative motions between the Pioneering Spirit and a platform, the more difficulties might be expected when connecting Pioneering Spirit to the platform. Also during pipeline installation the relative motions could cause difficulties. When the pipeline is connected to the vessel and the sea floor, the relative motion of the vessel with respect to the sea floor will induce motions of the pipeline. Those motions induce stress fluctuations in the pipe, which if too high will reduce the fatigue lifetime of the pipeline. In order to prevent damage, the relative motions have to be limited.

The dynamic behaviour of a floating structure is dominated by the combined actions of the wave induced forces and the inertia of the structure. One of the major boundary conditions for offshore operations is the sea state. Suppose that the maximum operation condition is known for some offshore operation project, to be able to conduct the operation with a maximum safety, a time period must be selected in which the maximum sea state is not exceeded. The sea state is in general characterized by statistical parameters such as significant wave height H_s, the peak wave period T_p and the mean wave direction θ_m. The statistical representation of an ocean surface is known as the directional wave spectrum. In chapter 2 this topic is explored in more details.

Forecasts of the sea state, obtained by numerical prediction models such as WAM, IFS and SWAN are continuously monitored on board vessels. These models give a predictions of the statistical parameters of a sea state (H_s, T_p, θ_m). The forecast data are usually updated every three hours, however these forecasts depend on a lot of variables and still remain uncertain. By means of measuring the real time wave characteristics it is possible to validate the forecast.

Currently, on board of Allseas vessels, a wave monitoring system is used to obtain an estimation of the sea state. It uses nautical radar images to analyse the ocean surface. The experience of Allseas is that the system provides reasonable measurements of the wave period and wave direction. But the estimated wave height is less reliable. Such observations can also be found in the literature [11].

2.2 Thesis objective

To be able to select a timeslot in which an offshore operation can be conducted safely, there is a need to improve the reliability of the real time wave height estimation. The wave height estimation is based on the estimated energy in the waves, since the wave energy is proportional to the square of the wave height. On board Allseas vessels, the H_s is estimated from the directional wave spectrum measured by the nautical radar. Chapter 5 gives a more detailed description of the measuring principle of the wave monitoring system. However, there is no unique relation between the radar images and the wave energy. Therefore there is a lack of accuracy.
In figure 2.1 the H_s measured by a WaveRider buoy is compared with the H_s estimated by wave monitoring system.

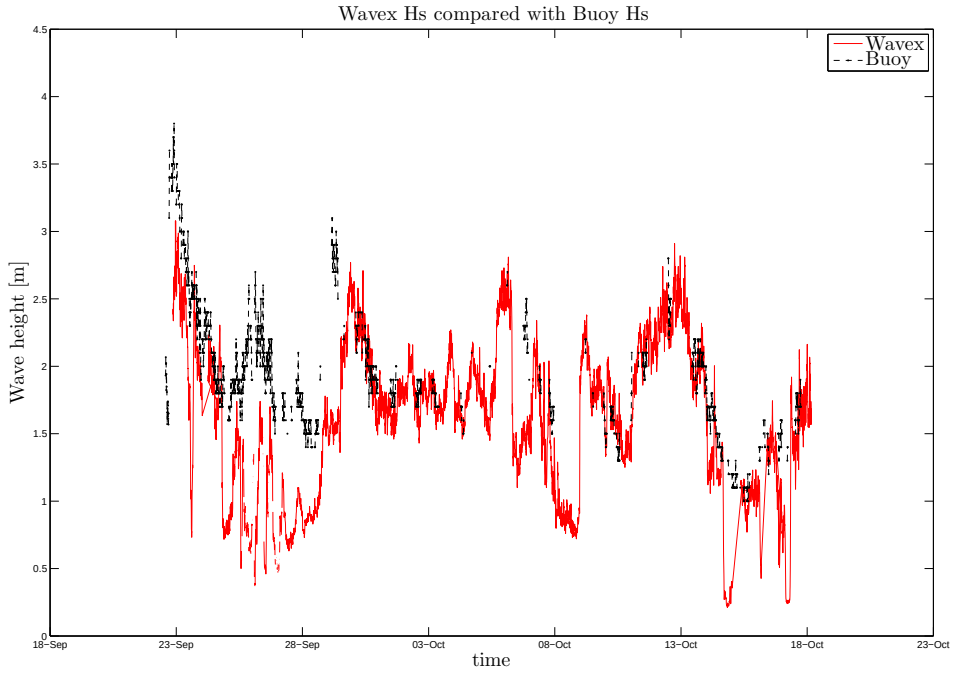

Figure 2.1: Measured wave height by different systems

The figure shows that the H_s measured by wave monitoring system deviate from the H_s measured by the WaveRider buoy. The objective of this thesis is thus as follows:

Improving the estimate of the amount of energy in a real time directional wave spectrum measurement without using in-situ instruments

To achieve this, it is investigated whether it is possible to combine different sensors to improve the estimated wave spectrum. To test and validate this a case study is performed for Allseas vessel Audacia.

2.3 Document structure

Chapter 3 describes the literature of the existing methods to estimate the directional wave spectrum without using any instruments deployed in the water. Basically those methods can be divided in methods which use vessel motion (Response based methods) and methods which use the radar as remote sensor (Radar based) to determine the directional wave spectrum.

In Chapter 4 the concept of data fusion is introduced. In this method, the vessel motions are combined with the wave field information extracted from radar images.

In chapter 5 the investigated methods are introduced. Two methods are investigated. The first methods combines the vessel motions with the directional wave spectrum given by wave monitoring system. The second method combines a down looking radar data with data from the conventional nautical radar. To validate those methods, a case study dataset is compiled.

In chapter 6 the results of the case study are given.

Chapter 3

Wave energy spectrum estimation

In literature there are basically two concepts to distinguish to determine wave energy spectrum with directional information, without using any equipment deployed in the water:

Response-based. In general a waveRider buoy is considered to be a reliable device for obtaining a directional wave spectrum of ocean waves, because of the well known dynamic behaviour. The concept of the wave rider buoy can also be applied on ships. In literature several papers exist [7],[8],[9],[5] which deal with the estimation of directional wave spectra from measured ship responses. This method is also known as the wave buoy analogy.

Radar image based. In the last few decades the phenomena that under various conditions signatures of sea surface were visible on nautical radar images is investigated. These so called 'sea clutter' were undesirable for navigation purposes and therefore generally depressed by filtering. In the 70s and the early 80s this sea clutter which is caused by the backscatter from the short sea surface ripples is used to provide a two dimensional wave spectrum, Alpers 1981. This development allows to analyse the sea surface in space and time with a resolution. Borge [1] has improved the empirical correlation in 1998, but still a calibration is needed to determine the significant wave height. In 2004 Dankert [3] claims to have developed a method to obtain a directional wave spectrum from the raw data of a nautical radar for which no calibration is required.

3.1 Wave energy spectrum

As the main objective of the thesis is to estimate the directional spectrum, a physical understanding of the sea surface elevation and wave induced vessel motions is required.

3.1.1 Wave frequency spectrum

In a surface elevation time record, the surface elevation is the elevation of the sea surface relative to the still water level. A wave in such time record is the profile of surface elevation between two zero-crossings. The wave height is defined as the vertical distance between the lowest and the highest surface elevation in a wave. The wave period is defined as the time interval between the start and the end of the wave.

It is known that any irregular wave time series can be made of an infinite sum of regular sine waves, each with its own amplitude, frequency and direction. This is the so-called superposition principle introduced first by St Denis and Pierson (1953). Hence, to distinguish the relative importance of the component sine wave, the directional energy density spectrum is introduced.

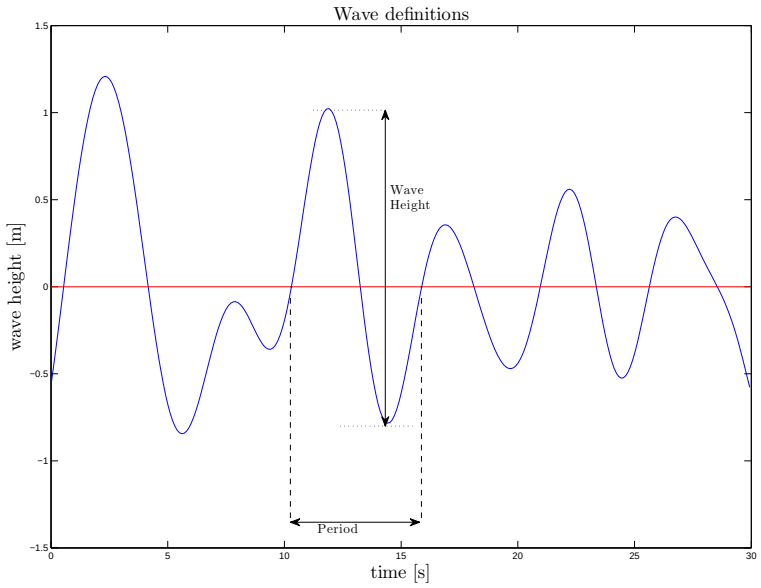

Figure 3.1: Wave definition

Consider a time record of the surface elevation at one location as a function of time, with a duration D (in seconds). The surface elevation can be reproduced as the sum of a large number of harmonic wave components, stated by the so called superposition principle.

$$\zeta(t) = \sum_{i=1}^{N} \zeta_{a_i} \cos(\omega_i t + \alpha_i) \tag{3.1}$$

where ζ_{a_i} is the amplitude and α_i the phase of each frequency $\omega = 2\pi_i/D$.

With spectral analysis it is possible to determine the values of the amplitudes and phases for each frequency ω. Describing waves in a wave record requires that the duration of the record is short enough to be stationary, but also long enough to obtain a somewhat reliable frequency resolution. The most commonly used compromise is using a duration between 15 and 30 minutes.
The phases can have any value between 0 and 2π without any preference, and since there is no interest in rebuilding the exact time record the phase spectrum will be ignored. The amplitude spectrum remains to characterize the wave record. This is called the random phase/amplitude model. From a statistical point of view not the amplitude spectrum, but the variance spectrum is used as the variance is proportional to the energy of the wave. Both the amplitude and the variance spectrum are based on discrete frequencies, where as nature does not select discrete frequencies. To represent nature in a more realistic way the variance of each frequency ω_i is distributed over frequency interval $\Delta\omega_i$ which result in the continuous variance density spectrum.

$$S(\omega) = \lim_{\Delta\omega \to 0} \frac{1}{\Delta\omega} S\{\frac{1}{2}\underline{\zeta_a}^2\} \tag{3.2}$$

3.1.2 Directional wave spectrum

The one dimensional variance density spectrum describes a single point surface elevation. To describe a moving wave the directional information has to be added. The wave frequency

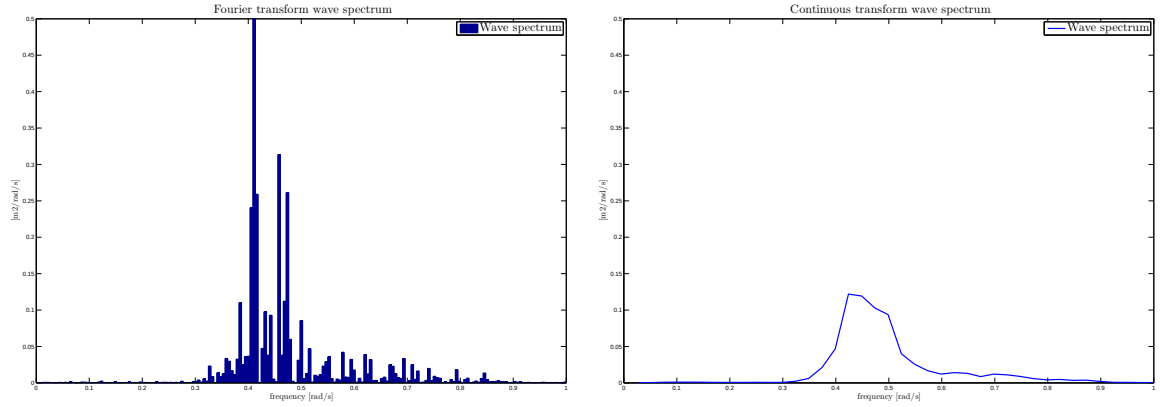

(a) variance spectrum

(b) variance density spectrum

Figure 3.2: Visualisation of random phase/amplitude model

spectrum is expanded by considering a wave propagating in the (x, y) space. In the same manner as in the one dimension time record, the two dimensional surface elevation can also be described with the sum of a large number of waves. The propagating direction θ is relative to the positive x-axis. The surface elevation for any position (x, y) is described in equation 3.3.

$$\zeta(x, y, t) = \sum_{i=1}^{N} \sum_{j=1}^{M} \zeta_{a_{i,j}} \cos(\omega_i t - k_i x \cos(\theta) - k_i y \sin(\theta) + \alpha_{i,j}) \tag{3.3}$$

where k is the wave number $k = \frac{2\pi}{L}$ and L the length of the harmonic wave and $\alpha_{i,j}$ contains the phase information.
The directional wave spectrum $S(\omega, \theta)$ can be obtained by multiplying the wave frequency spectrum with a directional spreading function $D(\theta)$.

$$S(\omega, \theta) = S(\omega) \cdot D(\theta) \tag{3.4}$$

The directional distribution is essentially the cross-section through the two-dimensional spectrum at a given frequency, normalised such that its integral over the directions is unity (Holthuijsen, 2009).

3.2 Wave energy spectrum estimation from response measurements

Estimation of the wave spectra based on measured ship responses can be split into two concepts, namely parametric modelling and non-parametric modelling. In the parametric method a pre-assumed directional wave spectrum is optimised by using the relation between the measured motion responses and the wave spectrum [8], [9]. The pre-assumed wave spectra are spectra similar to those of Jonswap, Pierson Moskowitz or the Ochhi Hubble. The main drawback, considering estimating wave spectra based on a parametric method, is that the real wave spectra have to be described with a restricted number of parameters. Further, the parametric method is a relative expensive one with respect to computational cost, since the solution is obtained from a non linear optimisation problem.
With the non-parametric method the directional wave spectrum is found 'directly' as the values

in a completely discretized frequency-direction domain without making prior assumptions. On-site wave spectra can be estimated on the basis of measured ship responses by use of Bayesian modelling, c.f. Iseki [5] and Nielsen [7]. Both concepts will be more explored in the following paragraphs.

3.2.1 Response amplitude operator

In previous section it is shown that the sea state can be described with a directional wave spectrum. In many cases vessel motions mainly have a linear behaviour with respect to the sea state, which means that there is a linear relation between the wave amplitude and the vessel motion amplitudes. Therefore it is possible to calculate the vessel response spectra if the wave spectrum is known. This also applies in reverse order. In all vessel motions are known, it should be possible to calculate the wave spectrum.

The effects of sea state upon the floating vessel motions are defined with transfer functions. The ratio between the wave amplitude and the response amplitude is also known as Response Amplitude Operators (RAO's). In equation 3.5 the relation between the directional wave spectrum $S(\omega, \theta)$ and the motion response ϕ_{mn} is described. The RAO_m and RAO_n are the linear transfer functions for motion m and n respectively. $S(\omega, \theta)$ is the input directional wave energy spectrum.

$$\phi_{mn}(\omega) = \int RAO_m(\omega, \theta)\, \overline{RAO_n}(\omega, \theta)\, S(\omega, \theta)\, \mathrm{d}\theta \tag{3.5}$$

The Rao's of a given ship are a function of wave period and encounter wave direction. The ship does not respond equally to waves with different encounter direction, even when wave period is the same. As you can imagine, the ship respond differently to stern waves than to beam waves.

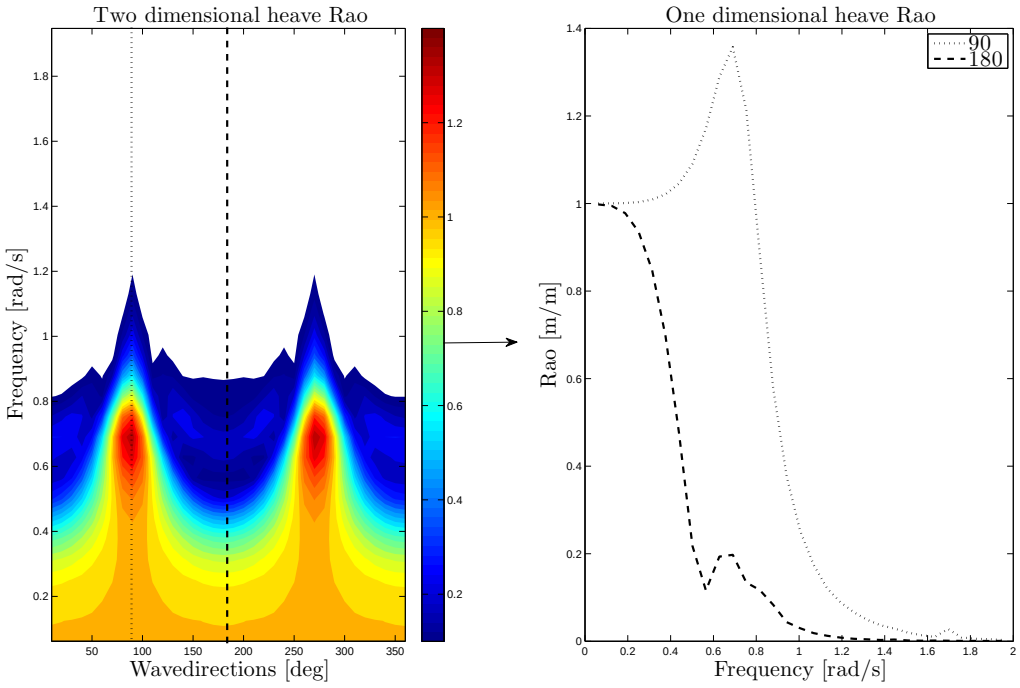

Figure 3.3: Heave Rao

In figure 3.3 this dependency is visualized. To illustrate, the values for two direction are shown. In the left-hand side plot two dashed lines are depicted, which stand for the wave encounter directions, respectively 90° and 180° . In the right-hand side plot the heave Rao is plotted for those two wave encounter directions.

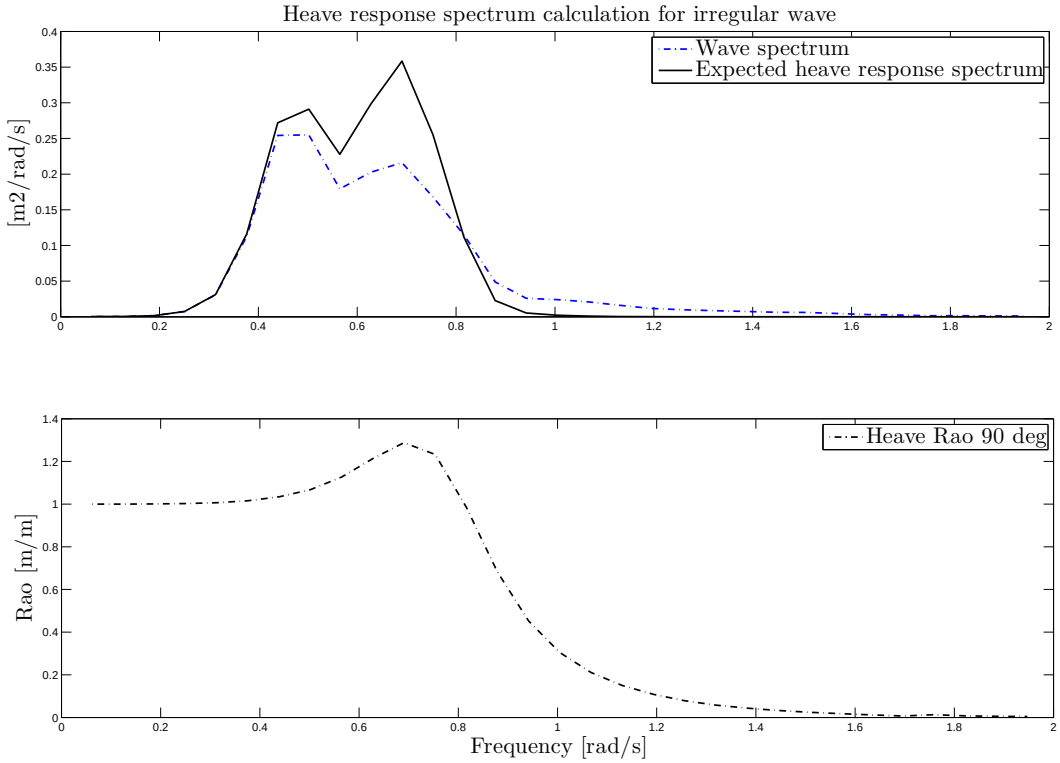

Figure 3.4: Heave response for irregular waves from 90°

To visualize the response calculation, suppose irregular beam waves. The wave direction is assumed to be exactly 90° with respect to heading of the vessel. In figure 3.4 the relation between the wave spectrum and the heave response is visualized. As can be seen the response the heave spectrum tend to follow the wave spectrum till approximately $0.4\,rad/s$ and for waves with higher frequency than $0.8\,rad/s$ the vessel motion is dominated by its mass and the waves are losing their influences on the vessel motion. In between the damping dominates the response. If the damping would be zero, the motion would go to infinity due to resonance.

3.2.2 Parametric modelling

This method assumes that the directional wave spectrum can be comprised in one parametrised known wave spectrum. Known parametrised wave spectra are considered to be reliable for describing the variation with frequency of the wave spectrum and the angular spread can be described with certain parameters. One of the possible pre-assumed bimodal parametric directional wave spectra proposed by Hogben and Cobb 1986:

$$S(\omega,\theta) = \frac{1}{4}\sum_{i=1}^{2} \frac{\left(\frac{4\lambda_i+1}{4}\omega_{p,i}^4\right)^{\lambda_i}}{\Gamma(\lambda_i)} \frac{H_{s,i}^2}{\omega^{4\lambda_i+1}} A(s_i)\cdot\cos^{2s_i}\left(\frac{\theta-\theta_{mean,i}}{2}\right)\exp\left[\frac{4\lambda_i+1}{4}\left(\frac{\omega_{p,i}}{\omega}\right)^4\right] \quad (3.6)$$

with H_s being the significant wave height, θ_{mean} the mean wave direction, λ the shape parameter, ω_p the angular peak frequency and s the spreading parameter and $A(s_i)$ a constant to normalise the area under the cosine function. Using the linear ship theory the vessel motion responses upon the spectrum $S(\omega, \theta)$ can be calculated:

$$\phi_{mn}(\omega) = \int RAO_m(\omega, \theta)\, \overline{RAO_n}(\omega, \theta)\, S(\omega, \theta)\, \mathrm{d}\theta \tag{3.7}$$

The main idea of the parametric modelling method is to perform an error calculation between the measured and the calculated response spectra. To distinguish the difference between starboard and port side entering waves at least one of the considered ship response motions has to be port/starboard symmetrical.

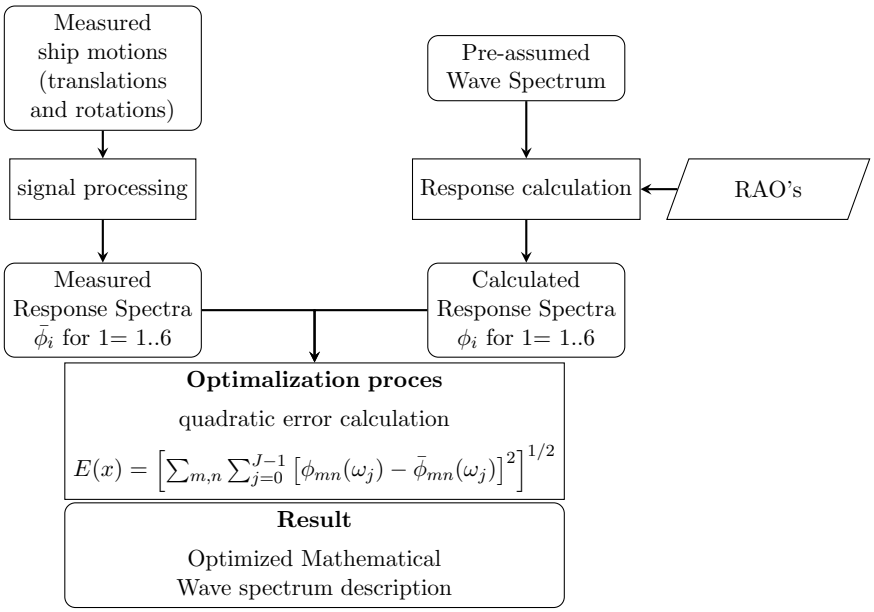

Figure 3.5: Flowchart of the parametric modelling

In parametric modelling the wave spectrum $S(\omega, \theta)$ is estimated through an optimisation. The result of the optimisation is a set of optimised wave parameters from the pre-assumed parametrised wave spectrum. The choice which parametrised wave spectrum to use depends on the set of parameters which have to be optimised and the sea states that have to be described *(uni-modal, bimodal,trimodal)*. The actual optimisation problem solution is established by minimising the difference between the left and right side of the equations. The quadratic error formula is given by equation 3.8:

$$E(x) = \left[\sum_{m,n} \sum_{j=0}^{J-1} \left[\phi_{mn}(\omega_j) - \bar{\phi}_{mn}(\omega_j)\right]^2\right]^{1/2} \tag{3.8}$$

For the minimisation a tool is required. In the literature there are different algorithms used to deal with the optimisation problem. As the minimisation problem has various local minima, a local minimizer will hardly converge to the true minima. In literature the Genetic optimisation algorithm or gradient search algorithm are proposed and utilised as a robust method to converge to the true minimum. If a good initial guess is available the local minimizer can be used. The

solution obtained by D. Nielsen and D.Stredulinsky is using a built-in function in MATLAB®, the so called *fmincon* function.

3.2.3 Non- parametric modelling

The main difference between the the parametric modelling and the non-parametric modelling is that the latter does not explicit assume that the true wave spectrum can be described by any know mathematical directional wave spectrum. Therefore the energy density is determined by using a number of discretized points. The Baysian method is used to model and solve the true wave spectrum.

3.3 Radar based wave spectrum estimation

The second concept is the radar image based method. The method of radar imaging is based on analysing the spatial structure of the radar image and its temporal evolution. Normally the radar is used to detect hard obstacles around the vessel. But since the radar transmitted wave length is in the order of centimetres, the sea surface ripples reflect the transmitted radar waves and modulate the radar backscatter. These reflected radar waves are modulated by larger structures, such as swell and wind sea waves. The pattern visible in the radar image is known as sea clutter. The modulation of the backscatter by ripples and the roughness of the sea surface is mainly caused by the following mechanism:

- *Hydrodynamic modulation:* Interaction of the ripples (capillary waves) with the longer waves leads to modulation of backscatter energy. Capillary waves tend to become localised on the crests of the swell waves, their amplitude will reach its maximum in this location. In the troughs there is virtually no signal reflected.
- *Tilt modulation:* Tilt modulation is a purely geometric effect which leads to a higher backscatter from a wave front which is directed towards the radar. A change in the local incidence angle leads to a change of the radar backscatter.
- *Partly shadowing:* this effect occurs when the higher waves hide the lower waves to the radar antenna illumination. No radar signal is assumed to be received from this zones.
- *Wind modulation:* As the backscatter of the ocean waves is primarily caused by the small scale surface roughness, which is strongly influenced by the local wind field and therefore the backscatter is modulated by wind.

Spectrum estimation

Each measurement consist of a time series of consecutive radar images. The higher the radar image resolution the higher the resolution of the estimated wave spectrum. However, the system is installed on a nautical radar with certain configurations and therefore the temporal resolution of the radar image is determined by the antenna revolution period. The spatial resolution is a function of the antenna length and the radar pulse length. The backscatter is digitized for further processing. Briefly wave spectrum estimation consist in the following steps:

- After measuring a sequence of 32 subsequent polar images, a subsection of the sequence of polar images is collected and converted to Cartesian images, see figure 3.6. It has to be realised that the azimuth (cross range) resolution is a function of range. High image resolution is required to measure short waves, while large Cartesian images are required

to measure long waves. As large Cartesian images and high resolution cannot be obtained simultaneously each Cartesian image set consists of two images, one image with high resolution in close range and one large image at long range with a lower resolution.

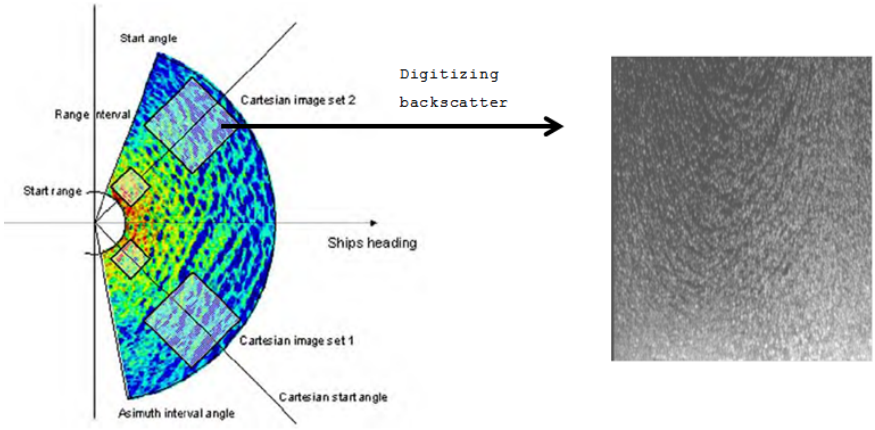

Figure 3.6: Backscatter digitzing of Orthogonal Cartesian image section of radar images (Wavex - principles of operation)

- The digitized subsection time series $\gamma(\mathbf{x}, t)$ (series of grey levels) is transformed into the spectral domain by using 3D FFT, resulting in an image spectrum $\chi_\gamma(\mathbf{k}, \omega)$. The image spectrum contains more than only wave spectrum information. In order to extract the wave information, the non-linear effects have to be removed. Ocean waves are assumed to be located close to the dispersion relation, these are separated from all other contributions by using a bandpass filter. A two dimensional wave number spectrum $\Psi_\gamma(\mathbf{k})$ is obtained by integrating over all frequencies.

$$\Psi_\gamma(\mathbf{k}) = \int_{-\infty}^{0} \chi_\gamma(\mathbf{k}, \omega) d\omega + \int_{0}^{\infty} \chi_\gamma(\mathbf{k}, \omega) d\omega \tag{3.9}$$

- Previous function is a multiplication of the wave number spectrum and its modulation mechanisms. The two dimensional wave number spectrum $\Psi(\mathbf{k})$ is obtained by applying the inverse of modulation transfer function $\mathcal{T}_\mathcal{M}(\mathbf{k})$.

$$\Psi(\mathbf{k}) = \mathcal{T}_\mathcal{M}(\mathbf{k}) \cdot \Psi_\gamma(\mathbf{k}) \tag{3.10}$$

- Once the two dimensional wave frequency spectrum is obtained, integrated wave variables can be derived.

In figure 3.7 the resulting two dimensional wave spectrum is plotted. The plot shows the energy distribution of frequencies and directions. The inner circles represent the wave period. The wave direction with respect to the heading of the vessel is visible at the outside circle.
For the energy distribution over frequencies the two dimensional wave energy spectrum is integrated over directions. In the left-hand side plot the two energy peaks can be seen. In the right-hand side plot the energy distribution over direction shows clearly the dominant wave direction.

The spectra obtained from the radar has values related to the grey levels. As the radar imaging mechanism depends on how the sea surface backscatters the emitted electromagnetic field

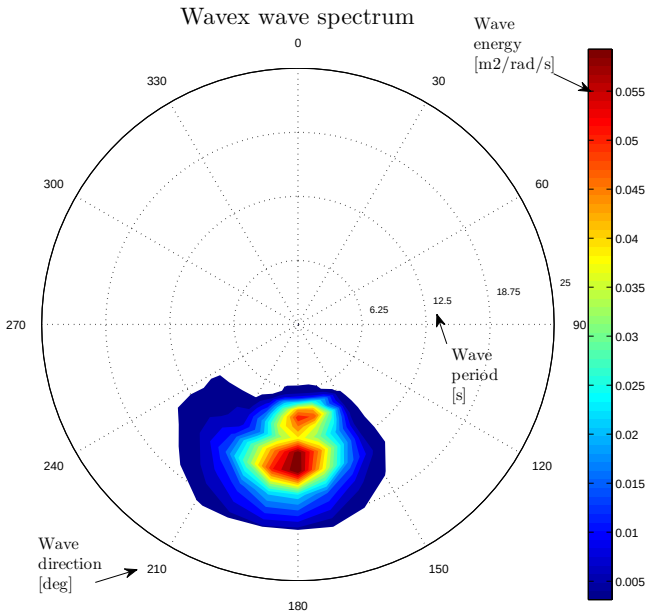

Figure 3.7: Radar based directional wave spectrum estimation

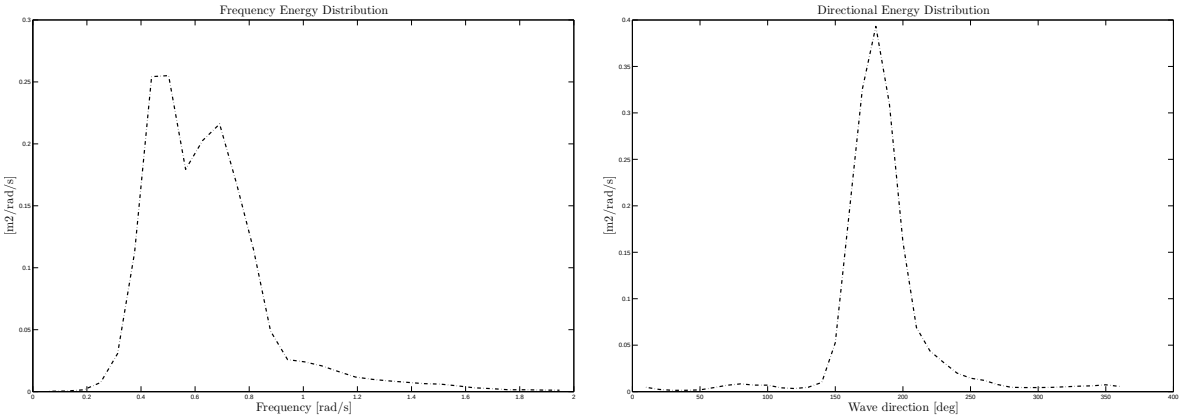

(a) Frequency energy spectrum

(b) directional energy spectrum

Figure 3.8: Energy distribution over frequency and direction for the two dimensional wave spectrum

which strongly depends on the local wind field, there is no unique relation between the radar backscatter and the wave height. Therefore, the system needs to be calibrated to provide an estimation of the absolute wave spectrum. However, the method used in Synthetic Aperture Radar (SAR) developed by Alpers and Hasselmann seems to be applicable for wave radar imaging. The marine radars can be calibrated in the same way as SAR. The basic idea is to relate the measured signal to noise ratio (SNR) to the significant wave height.

$$H_s = c_0 + c_1\sqrt{SNR} \tag{3.11}$$

with c_0 and c_1 are calibration constants.

3.3.1 Dankert's approach

Besides the currently used system, some other system exist to extract a wave spectrum. In this section another radar image based method, the method of Dankert, will be elaborated. Dankert presents an new empirical method for the determination of time series of ocean surface elevation maps from nautical radar image sequence [3] and [2].

Modulation mechanism

The modulation of the radar backscatter is mathematically described by the modulation transfer function, which is the sum of the geometrical effects of shadowing and tilt, hydrodynamic effects and wind modulation. Assuming that the surface elevation can be described by a Gaussian distribution, it is possible to describe the backscatter of each location (i.e. each pixel) of the radar image as a function of a mean backscatter $\bar{\sigma_0}$ for a longer period and a deviation $\delta\sigma_0$ from the mean. The value of the mean backscatter for a certain location represent the mean surface elevation. Assuming the Gaussian distribution, it belongs to the zero surface elevation, i.e. flat ocean surface. The formula is given in equation 3.12.

$$\sigma_0 = \bar{\sigma_0} + \delta\sigma_0 = \bar{\sigma_0} \cdot \left(1 + \int M\left(\vec{k}\right) \cdot e^{i\left(\vec{k}\vec{r} - \omega\left(\vec{k}\right) \cdot t\right)} d\hat{\eta}\left(k\right)\right) \tag{3.12}$$

The deviation from the mean represent a local and temporal change of the depression angle, which is assumed to be equal to the local ocean surface tilt. The method of Dankert is an extension of the existing methods and can be seen as an alternative to the inversion method used in the Wavex Wave Monitoring system.

Chapter 4

Data fusion

In previous chapter the methods to obtain a two dimensional wave energy spectrum were restricted to using one single measuring system. Data fusion, in case of wave spectrum estimation, is the process of combining multiple sensors with a known behaviour and relation between the output and the wave spectrum. In principle, any type of response signal, obtained as time series, may be utilised in the wave spectrum estimation as long as a linear complex-valued transfer function exists. In 2011 D. Stredunlinsky and M. Thornhill [11] developed a method to improve the shipboard wave spectrum measurement through fusion of the extracted wave spectrum from radar image sequences with measured ship motion response data.

DataFusion by Stredunlinsky

Since the normalized directional spectrum estimated by the radar based system is generally in agreement with the data of a wave buoy and the vessel motions have a direct relation with the energy in the wave spectrum, the idea of combining the radar data with the measured motions is attractive [11].

The uncorrected estimated wave spectrum $S(\omega, \theta)$ from the X-band radar is input to a response ship motion prediction program. Comparison of the measured ship motions with these prediction is used to scale the estimated wave spectrum. The method is visualized in figure 4.1.

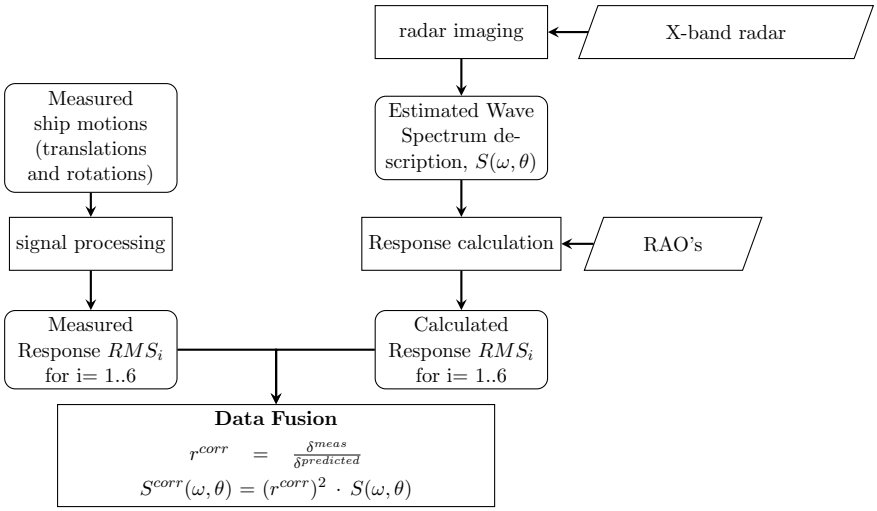

Figure 4.1: Flowchart Shipboard Wave Data Fusion method

If $\delta^{predicted}$ is one of these RMS motion components calculated using the wave radar input, and δ^{meas} is the RMS motion component measured during the same time period as the $S(\omega, \theta)$, the ratio between the measured and the predicted motion component can be determined. With the help of the obtained ratio the measurement of the directional wave spectrum can be corrected since the responses are a linear transformation of the wave excitations. In equation 3.7 the "corrected" directional wave spectral density $S^*(\omega, \theta)$ is given by:

$$S^*(\omega, \theta) = \left(r^{corrected}\right)^2 \cdot S(\omega, \theta) \tag{4.1}$$

with:

$$r^{corrected} = \frac{\delta^{meas}}{\delta^{predicted}}$$

As the responses are a linear transformation of the wave excitations, the scaled radar directional wave spectrum will provide a corrected response spectrum from the 'corrected' wave spectrum. So in essence, the method attempts to satisfy the condition that the measured responses match the calculated responses. However, the accuracy of different motion predictions can differ and errors in heading and frequency characteristics of the input wave radar spectrum can effect the motion differently, so the correction factor must be considered as a combination of different motion components ratios to improve the correction factor. If n motion components are considered and $\delta_i, i = 1, ..n$ and the correction ratio for the ith motion component is given by

$$r_i^{corrected} = \frac{\delta_i^{meas}}{\delta_i^{predicted}} \tag{4.2}$$

then the mean $r^{corrected}$ can be defined by

$$r^{corrected} = \sum_{i=1}^{n} \frac{r_i^{corrected}}{n} \tag{4.3}$$

Results by Stredunlinsky

The Shipboard Wave Data Fusion method by Stredunlinsky developed to improve the radar wave height estimation was tested and refined using post-trial analysis of data from 2006 and is demonstrated real time during the 2008 sea trials. Two wave buoys were deployed to measure the 'true' wave spectrum in the vicinity of the ship when the tests were executed. When the H_{mo} ranged between the 1 to 2 meters the SWDF method gave mean values 10 to 15% lower than the buoy measurements. The results of the mean significant wave heights were within 3% of the buoy measurements when the wave height was in the range of 3 to 5 meters.

Chapter 5

Thesis case study

5.1 Introduction

For this thesis project measurements were performed at Allseas vessel the Audacia. The Audacia is operational since 2007. The Audacia has a length of 225 meter and a width of 32 meter. Due to her length and shape the Audacia has a large pipe hold capacity of 14,000 tons and is less dependent on offshore pipe supply. The vessel is characterised by the stinger that is positioned on the bow and sails backwards when laying pipe.

Figure 5.1: Audacia pipelay vessel (Allseas.com)

5.2 Measuring systems on board Audacia

5.2.1 Miros Wavex

The Miros Wavex instrument analyses the conventional nautical radar images to extract directional sea state information. The working principle is already introduced in chapter 3.

5.2.2 Radac WaveGuide

The Radac WaveGuide instrument is installed below the helideck of the Audacia. The assumed location is 6 meters behind the aft perpendicular in the middle. In The instrument consist of a down looking radar and a motion sensor. As the wave height can be measured very accurate, it is possible to determine a reliable one dimensional wave surface elevation spectrum.

Instrument

The Radac Waveguide, a down-looking radar, is a sensor system to measure the single point surface elevation. The technology of the down-looking radar is quite common used in the process industry. The Radac Waveguide based on the Smartradar was originally developed for accurate

tank inventory measurements. This measuring method has proved to be very robust and hence the authorities approved this method for weight measurement in storage tanks and measures with an accuracy up to 1 mm [4]. However, sea surface measurements on a moving vessel differ from the still liquid level measurements in the storage tanks.

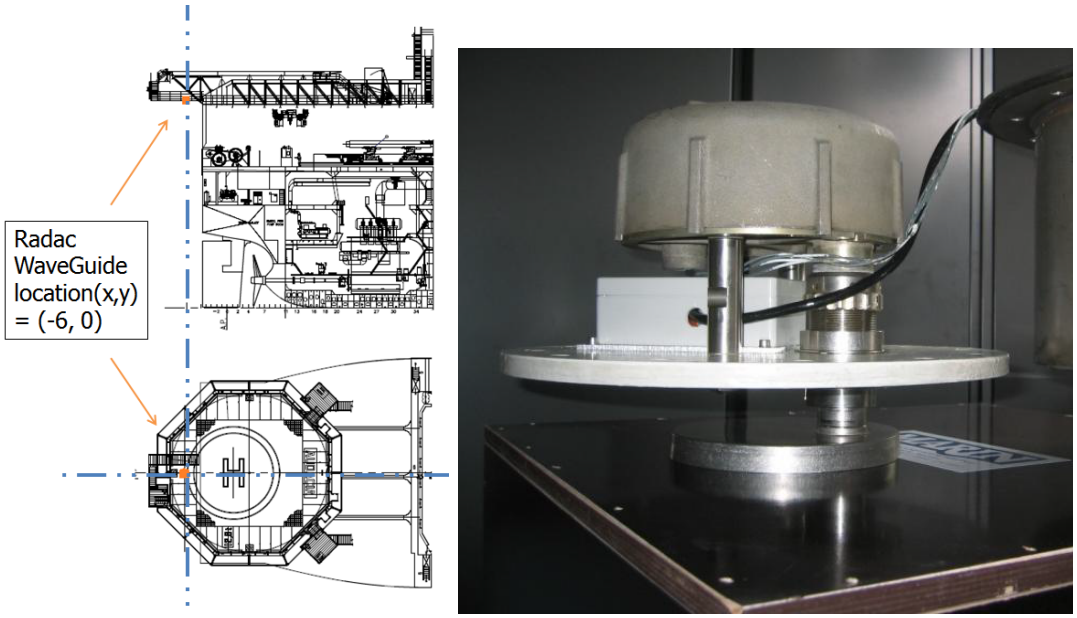

(a) Radac loaction (b) Radac device

Figure 5.2: Radac WaveGuide instrument and its location

The distance measurement between the Radac instrument and the water surface is based on the travelling time of the transmitted signal. A burst of signal pulses, that increases in frequency in a linear way, is transmitted towards the surface. The signal reflects on the water surface and is received by the antenna. As the propagation speed of the signal is determined by its frequency, the transmitted signal and the reflected signal are mixed. This results in a signal with a frequency equal to the frequency difference of the transmitted and received signal, the so called beat frequency. The travel time is determined by this frequency. The higher the frequency the larger the travelled distance.
At a moving vessel the measured distance has to be compensated for the vertical motion of the radar itself. Therefore a motion sensor is implemented to measure its three-dimensional motion. The sensor consist of a accelerometer and rate gyro based sensor. The sensor measures the three-dimensional motion with an accuracy of 1-2 cm. Combining those result in a time series of surface elevation with respect to its mean water level.

Spectrum estimation

From the measured time series a spectrum is calculated using the Fourier Transform. The measured time series has a resolution of $10\,mm$ and a sample frequency of 5 Hz. In figure 5.3 an example of Radac Waveguide spectrum is given. The spectrum has a frequency resolution of $0.01Hz$

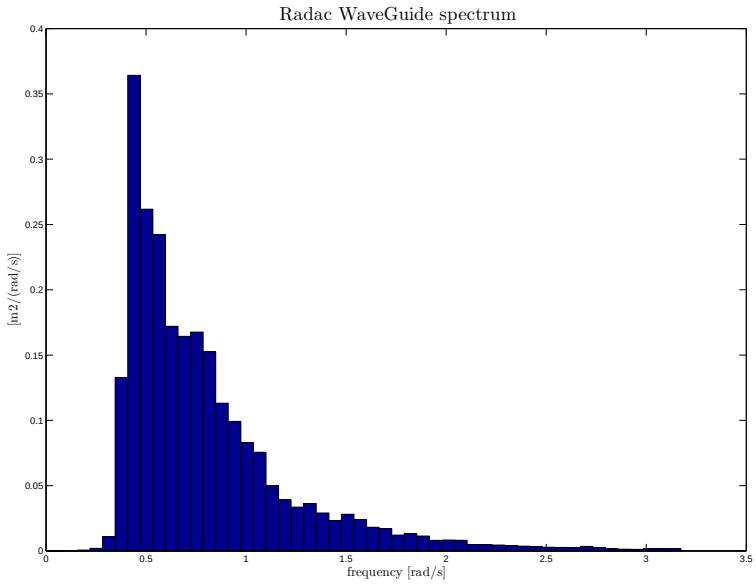

Figure 5.3: Radac measured wave spectrum

5.2.3 Ixsea Octans

The vessel motions are measured by the Ixsea Octans system. The heave, the vertical motion of the vessel is determined by the double integration of the vertical acceleration. Unfortunately, the vertical acceleration is measured with small bias due to the physical limitations of the sensors. Because of this bias, the double integration can diverge to infinity very quickly. In order to decrease this bias effect a high pass filter is used. If the motion sensor is moved following a sine or a combination of sinus, the surge, sway and heave output will follow this movement up to a period of 30 seconds. The motion measurement system is able to calculate the motion of an external monitoring point (see figure 5.4). This allows for instance that secondary monitoring points can be used to validate the measured motions.

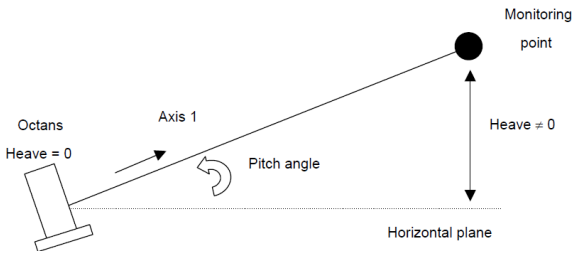

Figure 5.4: Monitoring principle (IXSEA, MU/OCTU/009)

Step one: Re-sampling

To be able to calculate a frequency spectrum from a time series, the time series has to be sampled uniformly. Since the output ixsea data is not uniformly logged, the time series is re-sampled.

Step Two: From Time Series To Motion Spectrum

The most common method regarding spectral analysis of time series is the Fourier Transform. It offers an easily applicable tool to calculate the spectral densities. The time series of the motion has a direct relation with the wave surface elevation time series, described with the linear ship theory. Therefore the vessel motion time series will also never be really stationary, and needs to be divided into segments that are each believed to be stationary. For a wave record a duration of 15 to 30 minutes is commonly used, which will be used for vessel motions as well.

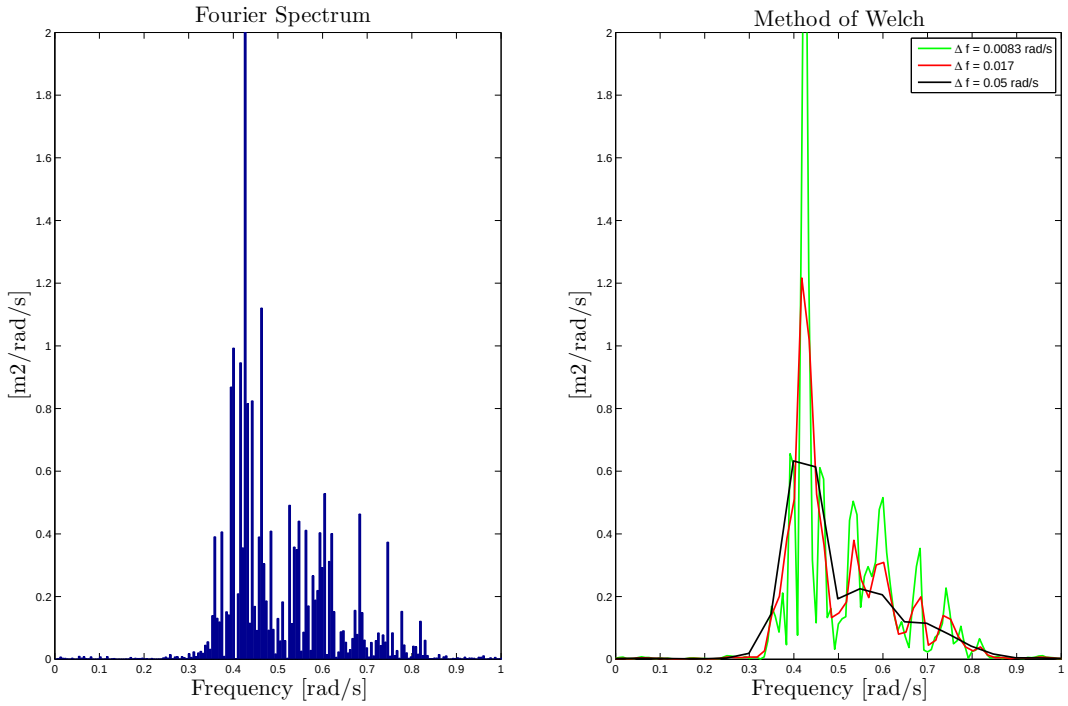

Figure 5.5: Wave spectrum estimation using method of Welch

Since the record has a limited duration and the Fourier Transform procedure uses linearly fixed frequencies the spectrum has a spiky distribution. There exist techniques to compensate for the limited time record. In general these techniques involve splitting the signal into overlapping segments and the use of window functions. However it has to be realised that the choice, such as the type of window, can greatly affect the result. It should be noted that the smaller the window size, the smoother the estimated spectrum and the more frequency dependent information might be lost. In exchange for frequency resolution there can be compensated for the limited duration. One of those methods is the method of Welch. Following Welch's method the original signal is divided into half overlapping segments. Each segment is multiplied with a Hann window $H[n]$.

$$H[n] = 0.5\left(1 - \cos\left(\frac{2\,\pi\,n}{M}\right)\right) \text{ for } 0 \leq n < M; \tag{5.1}$$

For each segment the discrete Fourier Transform is performed. A sensitivity analysis is performed to quantify how the number of segments affect the results. The results are visible in figure 5.5. It is clear that if the frequency resolution decreases, the spectrum is smoother due to averaging.

5.2.4 WaveRider

The wave buoy measures the waves by following the three dimensional motion of the water particles at the sea surface. Measuring the vertical motion of the buoy yields the wave height. For short waves relative to the buoy diameter, the boy does not follow the wave any more. For long waves, (low frequency waves) the buoy tend to follow the vertical motion of the wave. However, the mooring forces hinder the following of the wave. The extra mooring force depends on the wave amplitude. The measure in which following of the wave is hindered by the mooring forces is a function of the wave frequency.

5.3 Case study sea state

For research purposes measured data is logged for almost a month. Analysing all data would be impossible. Therefore in order to create a test case for the selected methods, a limited time period must be selected. In this chapter the main parameters like wave height, wave direction and wave period are visualized for the logged period.

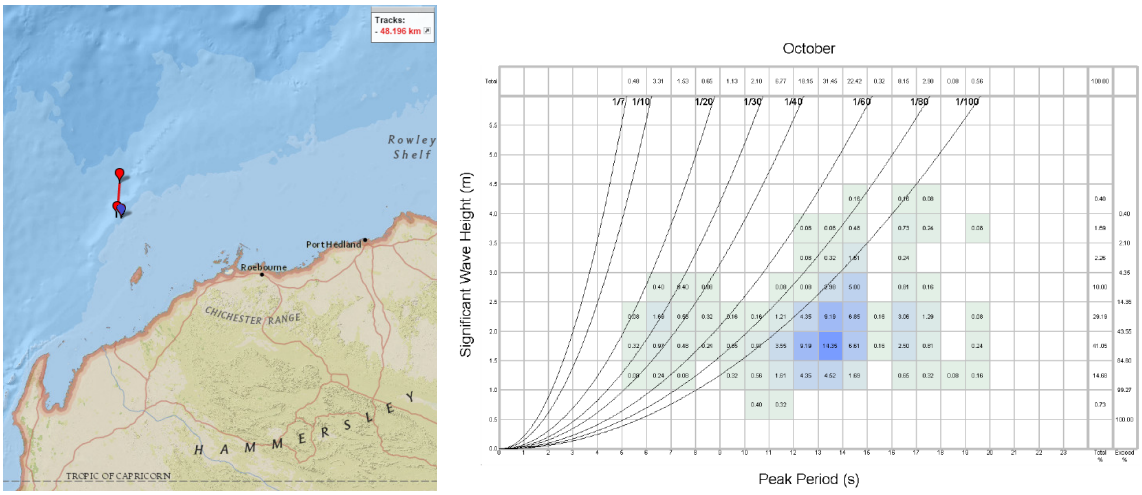

(a) Pipe laying track (marinetraffic.com) (b) Statistical wave data (FUGRO GEOS, C57022/7551/R0)

Figure 5.6: Vessel track and statistical data during measuring period

During this period the Audacia was laying pipe nearby the coast of Australia close to the Julimar Field. The installed pipeline track is plotted in figure 5.6a with red balloons. The location of the WaveRider buoy is shown in the same plot with a blue balloon.

In figure 5.6b the statistical data is based on wave buoy measurements from 1996 to 2010. From statistical data it is plausible that the measured peak wave period is between 13 and 14 seconds and significant wave height is expected between 1.5 and 2 meters.

Since statistical data does not contain any time dependent information, the value of the statistical data is limited. Since the wave data is not avaiable for the whole time period, a time period must be selected for which wave buoy data is available.

WaveRider compared with Wavex

In figure 5.7a the wave height measured by a WaveRider wave buoy is compared with the Wavex Wave Monitoring system wave height for almost one month. The black dots represent the 10 minute average measured by the buoy, the red line represents the wave height measured by the Wavex. As stated already in the thesis objective, the Wavex estimated wave height deviates at some periods and there is a need to be validated. In figure 5.7b the mean wave direction with respect to the vessel is plotted.

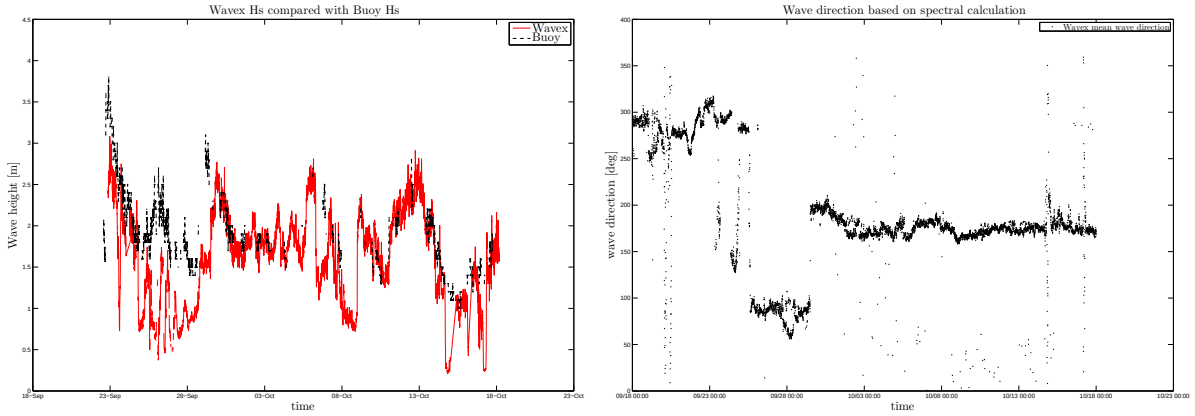

(a) One month of data

(b) 14 hours of data

Figure 5.7: Wave height comparison and mean wave direction

Unfortunately the wave buoy data is limited, hence a time period must be selected for which both are available. The selected time period is from 12AM to 2PM on October 14th.

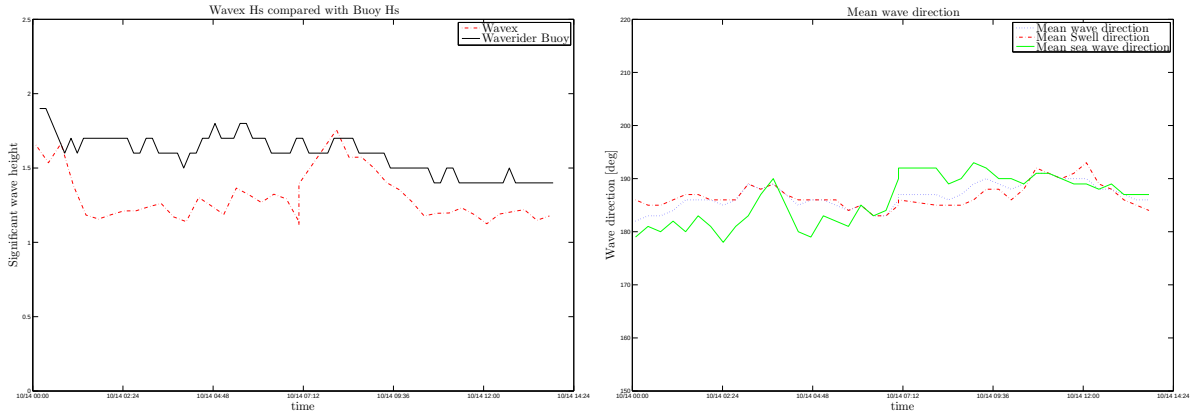

(a) Comparison wave height measurements

(b) Mean wave direction

Figure 5.8: Sea state wave height and wave direction during measurements

The significant wave height measured by the WaveRider buoy is almost constant during the selected time period, while the significant wave height by Wavex is deviating. In figure 5.8 the mean wave direction during the selected time period is plotted.
In the selected 14 hours of data the vessel sailed only 150 meters, so the forward speed can be neglected. The distance between vessel and the buoy is less than 2 kilometres.

5.4 Data fusion methods

In order to improve the directional wave spectrum estimations (2D wave spectrum) given by the X-Band radar used on board of the Audacia (Wavex from Miros), the possibility of using an extra measuring instrument to calibrate the energy is investigated. Two measuring devices are considered.

- A down looking radar (Radac WaveGuide), installed below the helideck of the Audacia, measures the single point surface elevation (1D wave spectrum) in vicinity of the vessel.
- The MRU sensors(Ixsea Octans), which measure the wave induced vessel motions.

5.4.1 Wavex combined with Radac

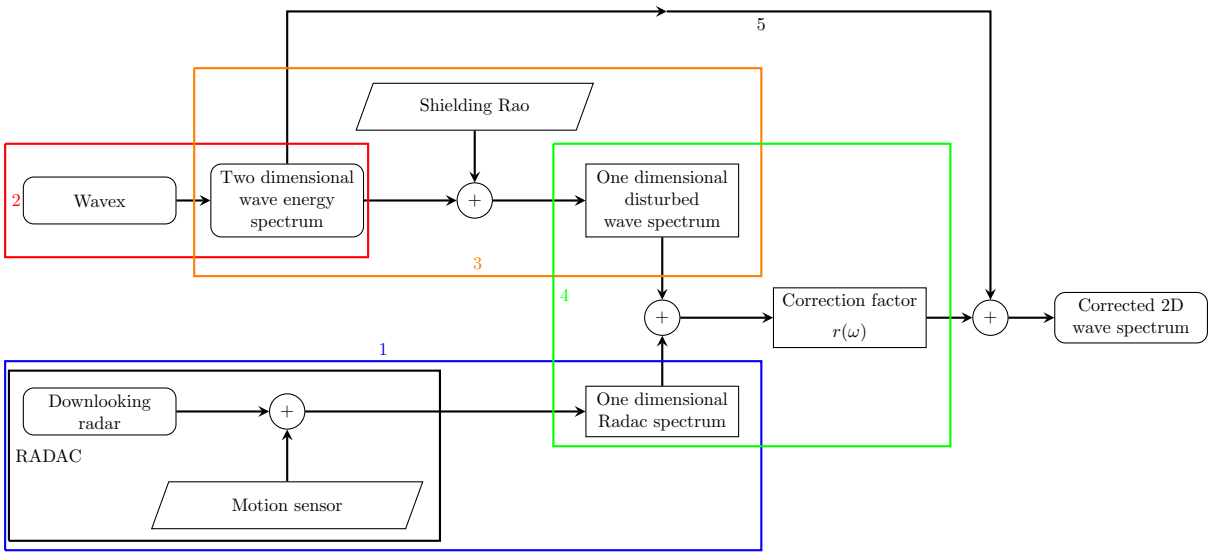

Figure 5.9: Flowchart Radac WaveGuide DataFusion method

The Radac WaveGuide Data Fusion flowchart describes the steps which have to be taken to correct the Wavex Wave Monitoring system measurement. All steps will be elaborated.

Step	**Colour**	**Process**
1	Blue	Processing Radac WaveGuide data to 1D wave spectrum
2	Red	Processing Wavex data to 2D wave spectrum
3	Orange	Determining shielded wave Rao's, Calculating 1D wave spectrum.
4	Green	Calculating the energy per frequency bin.
5		Correct the two dimensional Wavex spectrum

In this method the wave frequency spectrum given by Radac is combined with the directional wave spectrum given by Wavex. The wave frequency spectrum obtained by the downlooking radar is used to calibrate the energy in the directional wave spectrum obtained by Wavex. To calibrate the amount of energy in the directional wave spectrum first the data have to be made comparable.

As the Radac WaveGuide is installed below the helideck of the Audacia, the sea surface elevation in disturbed by the presence of the ship. The ship affects the wave field at the measuring location in two ways. First, incoming waves reflect on the hull, which could either shield the measuring area or amplifying the waves in the measuring area. As you can imagine, the extent in which the ship deform the wave spectrum depends on the measure in which the wave is hindered to arrive at the measuring location. Since the Radac WaveGuide provide a single point wave spectrum without any knowledge about wave direction, it is impossible to know in which measure the wave frequency spectrum is disturbed. Fortunately, the wave direction information extracted from conventional radar images may assumed to be reliable. To make the data comparable, the Wavex directional wave spectrum is translated to this disturbed measuring location, taking into account all contributions of disturbance.

Assuming the fluid to be ideal and irrational, the linear velocity potential can be used to describe waves and their effect on an oscillating rigid body floating in such waves. Using this theory it is possible to translate the directional wave spectrum given by Wavex to the disturbed location below the helideck. In this section a glimpse of the theory behind the fluid point Rao is given.

Potential function

The potential function of a fluid flow may be separated into a contribution from the radiation waves due to the six modes of vessel motion, the incident wave field and the diffracted or scattered wave field. Since the system is assumed to be linear the potential can be considered to be a combination of two separate problems.

1. Floating vessel moving in the flat water surface. The vessel motions will cause the fluid to react on the body and causes radiation forces. The forces can be written as a function of the motion and are commonly written in terms of added mass and wave damping.

2. Fixed vessel being subjected to regular incident waves. The wave exciting forces and moments can be broken down into two components, the Froude Krylov and the wave diffraction forces.

So the potential for a certain location may be written as a summation of the incident wave, diffracted and the radiation waves, see equation 5.2.

$$\Phi(X,Y,Z)\, e^{-i\omega t} = \left[(\Phi_I + \Phi_d) + \sum_{j=1}^{6} \Phi_j x_j \right] e^{-i\omega t} \tag{5.2}$$

where:

Φ_I	=	Incident wave potential
Φ_d	=	Diffracted wave potential
Φ_j	=	Potential due to j^{th} motion
x_j	=	motion j (per unit wave amplitude)
ω	=	Frequency of incident wave

The velocity potential can be used to describe the velocities in the fluid anywhere. To describe the sea with the velocity potential it has to fulfil a number of boundary conditions. The first boundary condition is that there should no water penetrate trough the seabed. If the water depth is h, this leads to:

$$\frac{\partial \Phi}{\partial z} = 0 \text{ for z = -h} \tag{5.3}$$

At the free surface the fluid velocity of a water particle must be equal to the velocity of the free surface:

$$\frac{\partial \Phi}{\partial z} = \frac{\partial \zeta}{\partial t} \text{ for z = 0} \tag{5.4}$$

The radiation term of the potential must decay to zero when the distance R to the body become large:

$$\lim_{R \to \infty} \Phi = 0 \tag{5.5}$$

Using the software packet AQWA from Ansys it is possible to determine the relation for any given location between the undisturbed wave field and the wave field due to the radiation and diffraction. The so-called fluid point Rao is a function of location (x, y), wave direction θ and wave frequency ω.

To visualize the disturbance at the measuring location of the Radac WaveGuide, the wave convention is plotted in figure 5.10. The wave direction is defined as coming from relative to the heading. So stern waves are waves coming from 180°, waves approaching at starboard are defined as waves with wave direction 90°. Said that, based on logical it is possible to predict the influence of the vessel on the undisturbed wave spectrum at location of the measuring point of the Radac WaveGuide.

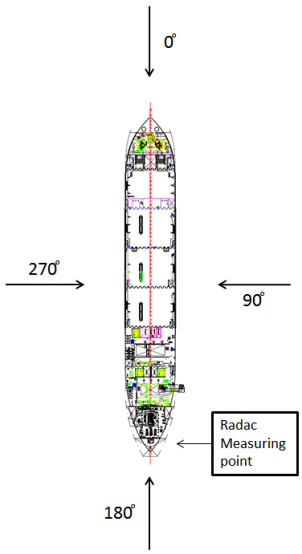

Figure 5.10: Wave direction convention

Long head waves are not affected by the presence of the vessel. Short head waves however will vanish as the vessel absorb their energy. So it is expected that the fluid point Rao for waves coming from 0° for low frequency waves tend to 1, and decrease for increasing wave frequency. For stern waves the waves reach the measuring point before reflecting to the ship hull. At some frequency the vessel reflect the waves in phase with the incoming waves and the wave amplitude increases. For beam waves the effect is more difficult to imagine. The waves at the measuring

point are a superposition of the undisturbed waves and the diffracted and radiated waves, so it is expected that the all frequencies remain present and none will get absorbed completely. In figure 5.11 the affect of the ship is plotted for all wave directions.

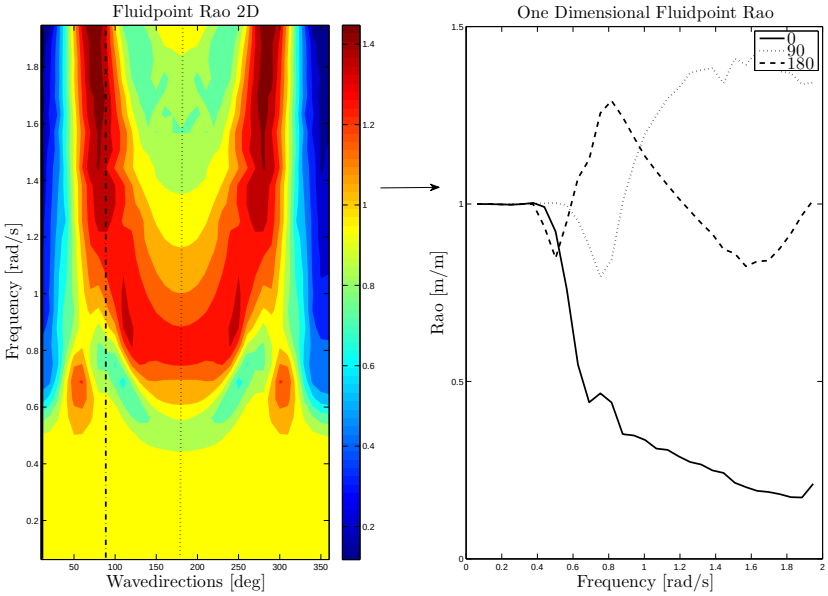

Figure 5.11: Fluidpoint rao for different wave directions

Making data comparable

Using the fluidpoint rao it is possible to determine the single point wave frequency spectrum at any location. Using the equation 5.6 it is possible to calculate the single point wave spectrum.

$$S_{(x,y)}(\omega) = \int \left(RAO_{(x,y)}(\omega,\theta)\right)^2 S(\omega,\theta)\,\mathrm{d}\theta \tag{5.6}$$

where:

$S_{(x,y)}(\omega)$	=	Disturbed wave frequency spectrum at location (x,y)
$RAO_{(x,y)}(\omega,\theta)$	=	Fluidpoint rao for location (x,y)
$S(\omega,\theta)$	=	Undisturbed directional wave frequency spectrum

Frequency dependent scaling

In figure 5.12 the wave frequency spectrum for location (x, y) determined using different instruments are plotted for an arbitrary 20 minutes of data. The ratio between the Radac wave frequency spectrum and the wave frequency spectrum determined using the undisturbed Wavex spectrum and the potential theory, can be used to determine for which frequencies the energy was not estimated correctly by Wavex.

$$r(\omega) = \int_{\omega-\Delta\omega}^{\omega+\Delta\omega} \frac{Radac(\omega)}{S_{(x,y)}(\omega)}\,d\omega \tag{5.7}$$

This frequency dependent ratio can be used to correct the estimated amount of energy at each frequency of the directional wave spectrum. It has to be realised that the amount of

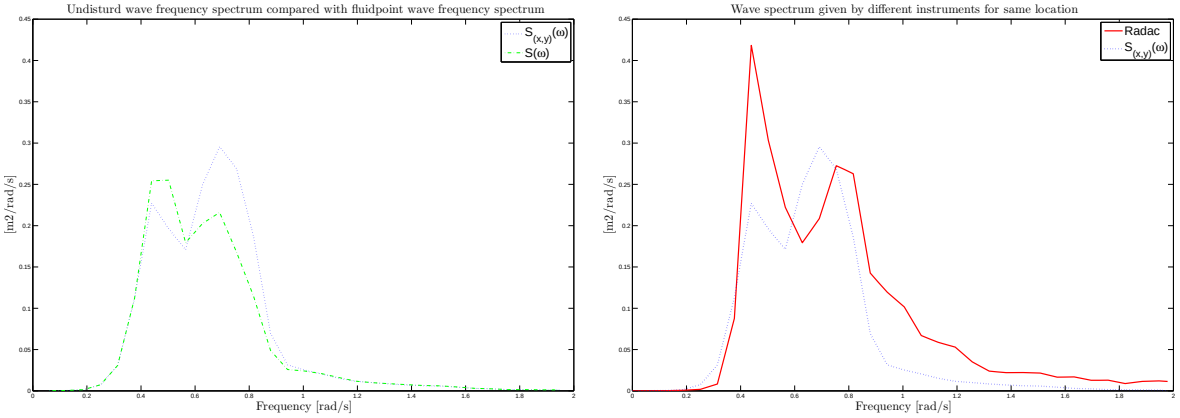

(a) Fluidpoint spectrum

(b) Radac compared with Wavex for same location

Figure 5.12: Potential theory applied to create comparable data

energy per frequency in the wave frequency spectrum is a summation of the energy distributed over all directions, the directional distribution of the energy is not corrected. The directional distribution of energy is assumed to be in agreement with the data of a wave buoy, as observed by D.Stredunlinsky [11].

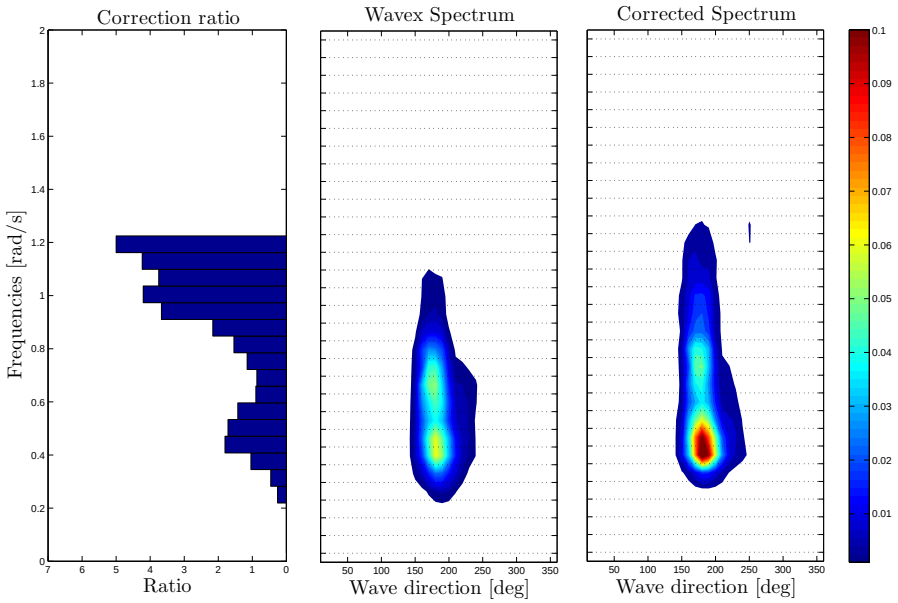

Figure 5.13: Visualization of Wavex correction

In figure 5.13 the result for this correction is shown. In the left-hand side plot, the correction ratio par frequency are visualized. In the plot in the middle the original wave spectrum for the same time period and in the right-hand side plot the result of its correction.

5.4.2 Wavex combined with Octans

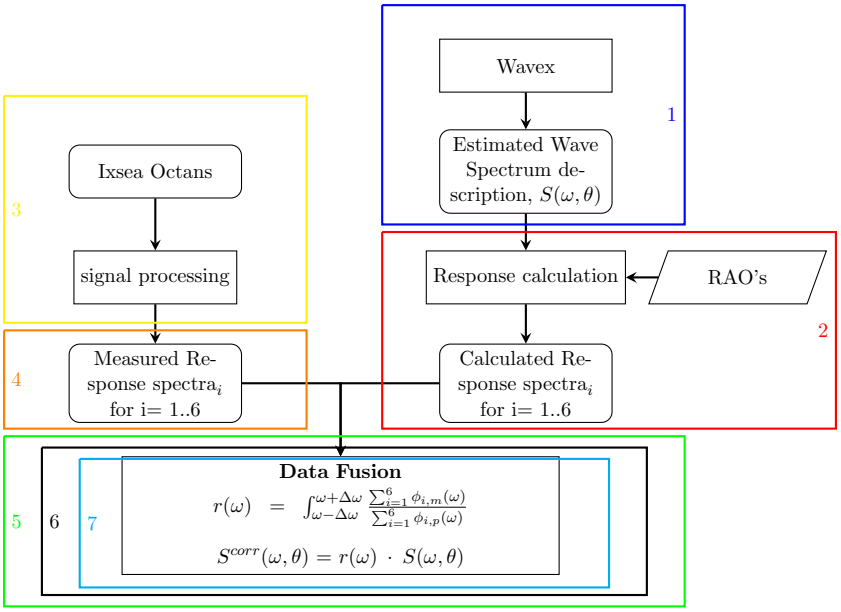

Figure 5.14: Flowchart Shipboard Wave Data Fusion method

Step	Colour	Process
1	Blue	Processing Wavex Data to frequency wave spectrum
2	Red	Calculate vessel responses based on Wavex spectrum
3	Yellow	Analysing vessel motions
4	Orange	Perform spectral analysis.
5	Green	Calculating the energy per frequency bin.
6	Black	Determining a frequency dependent ratio for each motion.
7	Cyan	Correct the two dimensional Wavex spectrum

In this method the measured wave induced vessel motions measured by motion sensors (Ixsea Octans) are combined with the directional wave spectrum given by Wavex. In order to use the ship response motion spectra to correct the directional wave spectrum given by Wavex, the have to be comparable. This means that the directional wave spectrum should be converted to motion spectra. In chapter 3 the linear relation between incident waves and vessel response was introduced. The first order vessel response motions can be calculated using the motion raos.

Correcting for the amount of energy in the estimated directional wave spectrum by using ship motions can be done in different levels.

- **RMS scaling** Using the ratio between the total amount of energy in measured response spectrum and the total amount of energy in the estimated response spectrum based on Wavex wave spectrum.
- **Frequency dependent scaling** Comparing the amount of energy in each frequency interval of the motion spectrum, following by scaling the amount of energy in each frequency band separately.

RMS scaling

D. Stredunlinsky suggested to compare the RMS of the measured response spectra with the RMS of the measured motion spectra. The Root Mean Square of any frequency spectrum can be calculated with equation 5.8.

$$RMS = \sqrt{\int_0^\infty S(\omega)\, d\omega} \tag{5.8}$$

The ratio between the RMS of the calculated response spectrum and the RMS of the measured response spectra is a measure of the ratio between the energy in the those spectra. He used this ratio to scale the wave spectrum. His approach attempts to satisfy the condition that the calculated response spectrum matches measured response spectrum by scaling the entire spectrum with the same correction ratio.

However, this approach has a few drawbacks. The entire wave spectrum is scaled with the ratio between the calculated RMS and measured RMS, but since the vessel only respond to a limited range of frequencies this relation does not give any information about the frequencies outside the response range.

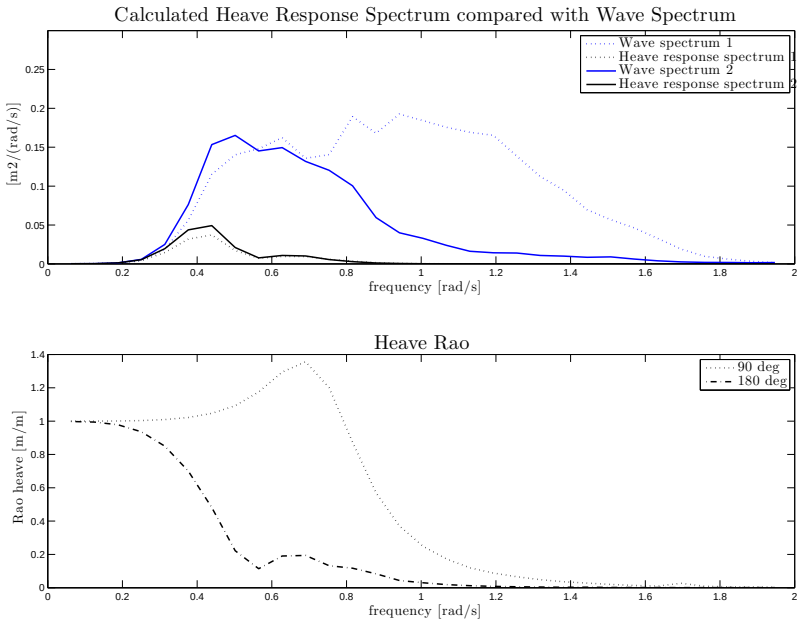

Figure 5.15: Response spectra related to wave spectra

In figure 5.15 this phenomena is visualized. It can be seen that even when the wave frequency spectrum for the different time stamps differ a lot, the heave response spectrum is quite similar. So therefore the range of frequencies that can be corrected is limited to the frequency range where the vessel respond to the wave excitations. The vessel's heave response gives an idea which range can be used. It has to be realised that this range depend on the direction of the waves since for vessel response depend on wave direction. This leads to the second method, frequency dependent scaling.

Frequency dependent scaling

Using a frequency dependent scaling factor was already used in the data fusion of the Wavex and Radac instruments, but there are two differences. Since the Ixsea Octans measures the motions of the vessel in 6 degrees of freedom, multiple vessel response spectra could be used to calibrate the amount of energy in each frequency.

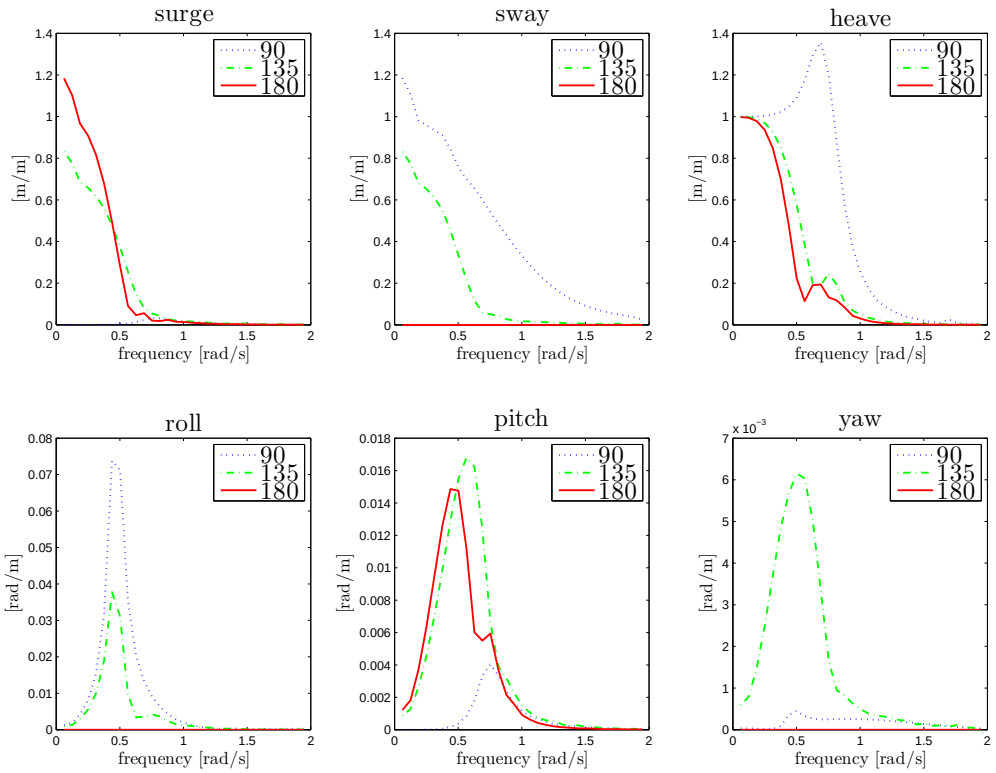

Figure 5.16: Audacia Raos

Since the response spectra is assumed to have a linear relation with wave spectrum it is valid to determine a scaling factor.

$$r(\omega) = \int_{\omega-\Delta\omega}^{\omega+\Delta\omega} \frac{\sum_{i=1}^{6} \phi_{i,m}(\omega)}{\sum_{i=1}^{6} \phi_{i,p}(\omega)} \tag{5.9}$$

with:

$\phi_i(\omega)$	motion i response motion spectrum
m	measured by motion sensors
p	predicted based on Wavex directional wave frequency spectrum

To visualize the comparison between the measured and the calculated response spectra, an arbitrary 20 minutes of data is analysed. The measured motion time series is plotted in blue. For the same time period, based on the Wavex wave spectrum, the expected vessel response is calculated using the linear relation between incident wave amplitude and vessel response motion amplitude.

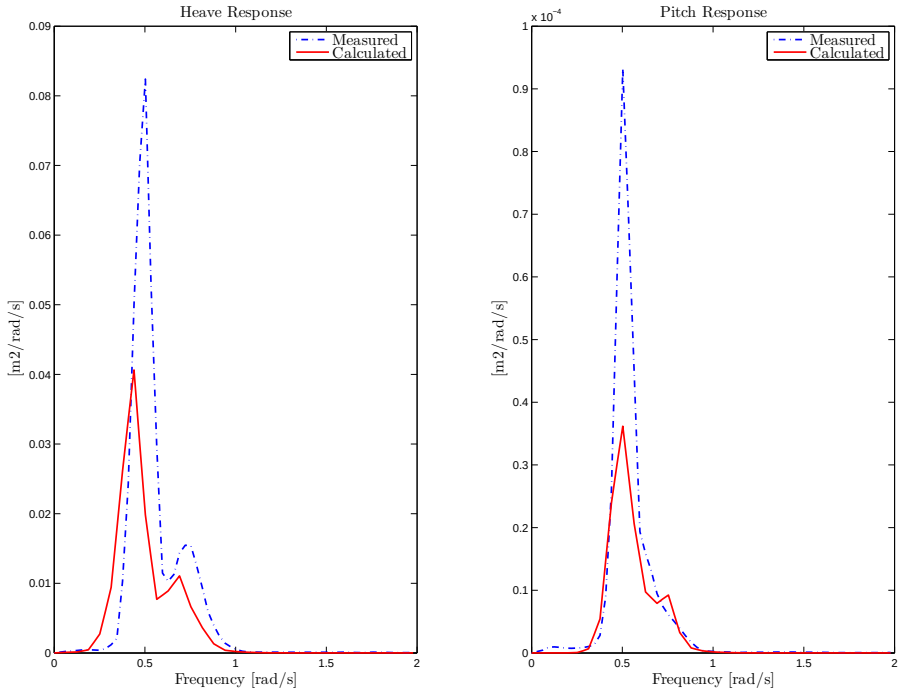

Figure 5.17: Measured response calculation and Calculated response

This calculated response spectra is called the predicted response spectra from now on. In addition to the data fusion of Wavex and Radac data, multiple motion measurements could be used to determine the frequency dependent ratio. The resulting frequency dependent ratio can be used to correct the estimated amount of energy at each frequency in the directional wave spectrum given by the Wavex.

Chapter 6

Results

In this chapter the results are presented for the the two data fusion concepts. In the first section the results of using the Radac as an extra measuring instrument are treated. In the second section the Wavex is combined with the measured vessel motions.

6.1 Data fusion between Wavex and Radac

6.1.1 Results

In order to validate the results of combining the Wavex with the Radac measurements, two validation layers can be found.

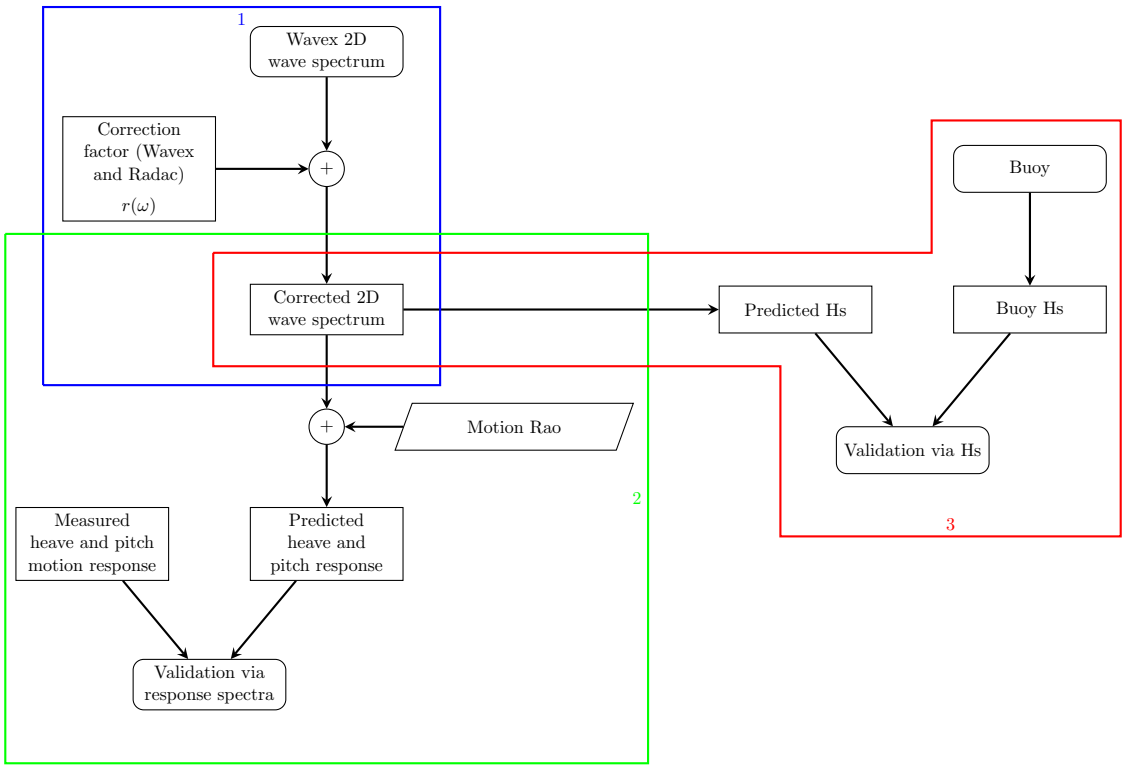

Figure 6.1: Flowchart Radac WaveGuide Validation

First, the Hs is calculated from the corrected Wavex spectrum using spectral calculation and compared with the measured Hs by the WaveRider wave buoy in the field (see number 3 in

flowchart). Second, using the motion raos the vessel response spectra are calculated from the corrected Wavex wave spectrum and compared with the measured motion spectra (see number 2 in flowchart). In figure 6.2 the Hs based on the corrected wave spectrum is compared with the WaveRider buoy is plotted.

Figure 6.2: Result of Wavex Correction

The significant wave height is only a measure of the amount of energy in the entire frequency range. However, the extent in which the two dimensional wave spectrum has changed is more important, the main purpose of knowing the directional wave spectrum is to be able to calculate the vessel responses. In figure 6.3 the two dimensional wave spectrum is plotted in a polar plot.

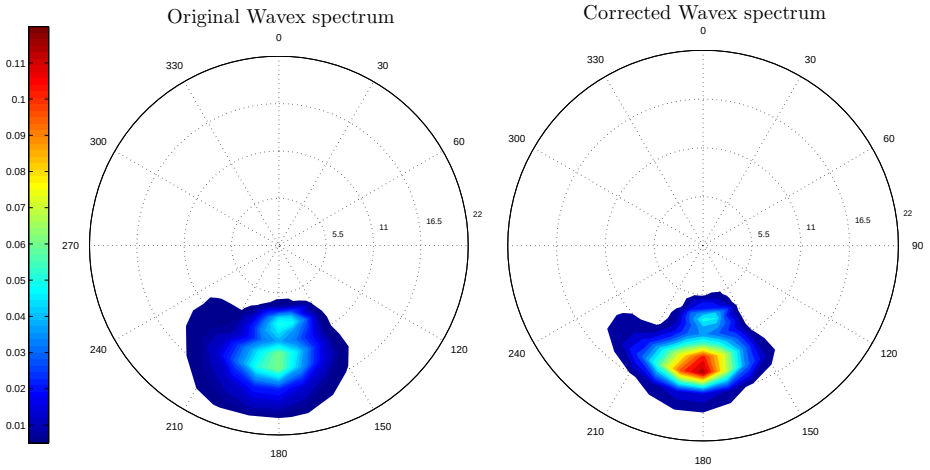

Figure 6.3: Correction visualized in two dimensional wave spectrum

The directions represent the approach angle with respect to the vessel heading. The inner circles represent the wave period. So in the original Wavex spectrum the mean wave approach angle

is around 180 degrees and the peak energy period is approximately 13 seconds. The amount of energy and its distribution is visualized with colors. The result of the correction is plotted in the right-hand side polar plot. It can be seen that energy is added, especially in the low frequency waves.

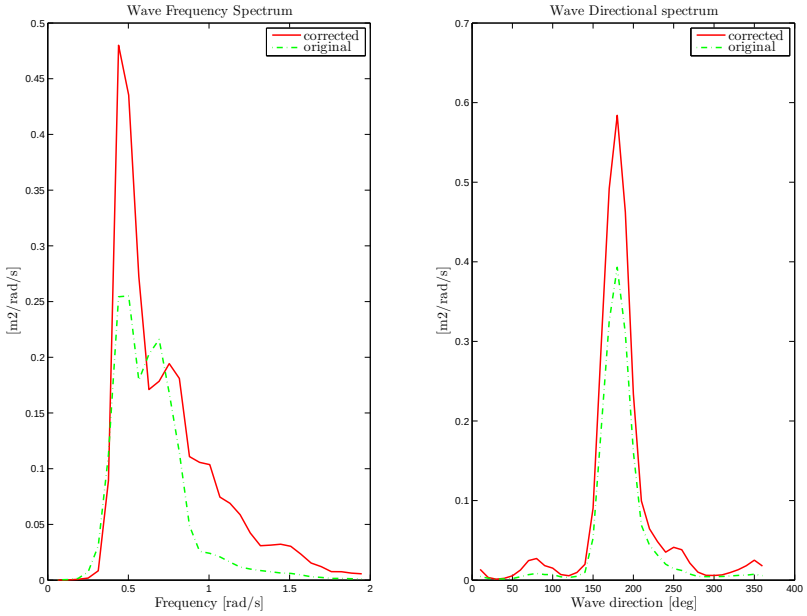

Figure 6.4: Correction visualized in one dimension

In figure 6.4 the energy distribution over frequency (figure 6.4a) and over direction (figure 6.4b) is plotted.

For the second validation layer the vessel motion spectra are calculated based on the corrected directional wave spectrum. In the comparison with the Hs the amount of energy in the entire wave frequency spectrum was validated. The amount of energy in the entire frequency range does not validate its energy distribution over frequencies.

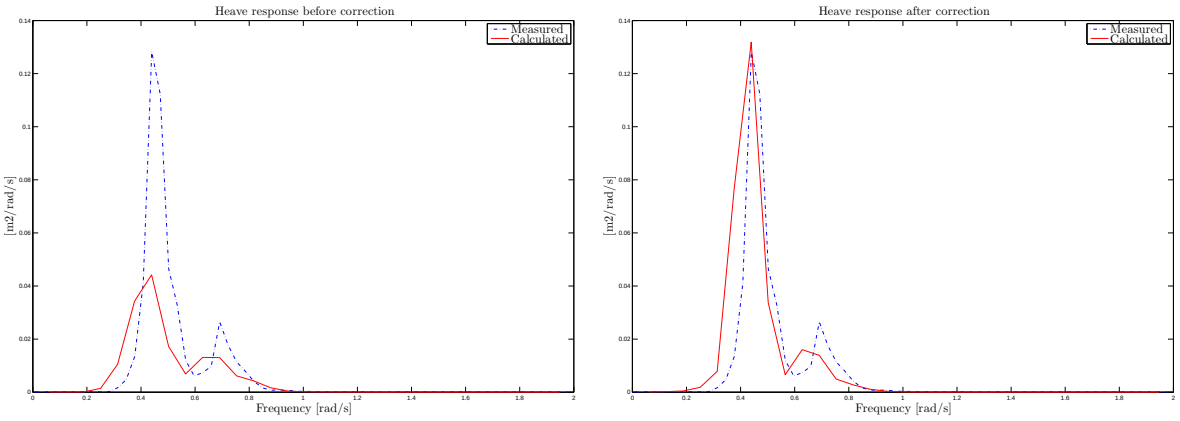

(a) Heave motion spectra before correction

(b) Heave motion spectra after correction

Figure 6.5: Improvement heave motion prediction visualized after correction with Radac data

If the calculated vessel motion response has a strong correlation with the measured vessel response motion based on the corrected directional wave spectrum, it is plausible that correction meets two conditions. First, the amount of energy in the frequency range in which the vessel respond to the waves is improved. Second, as the vessel motion rao's are strongly dependent on wave direction, it is plausible that the directional distribution estimated by the Wavex was in agreement with the true directional wave energy distribution.
In figure 6.5 the motion heave response spectra before and after is plotted. In blue the measured vessel motion response spectra. In red the calculated response spectra based on the Wavex directional wave spectrum before the data fusion. The heave response calculated based on the corrected directional wave spectrum has a strong correlation to the measured heave response spectrum.

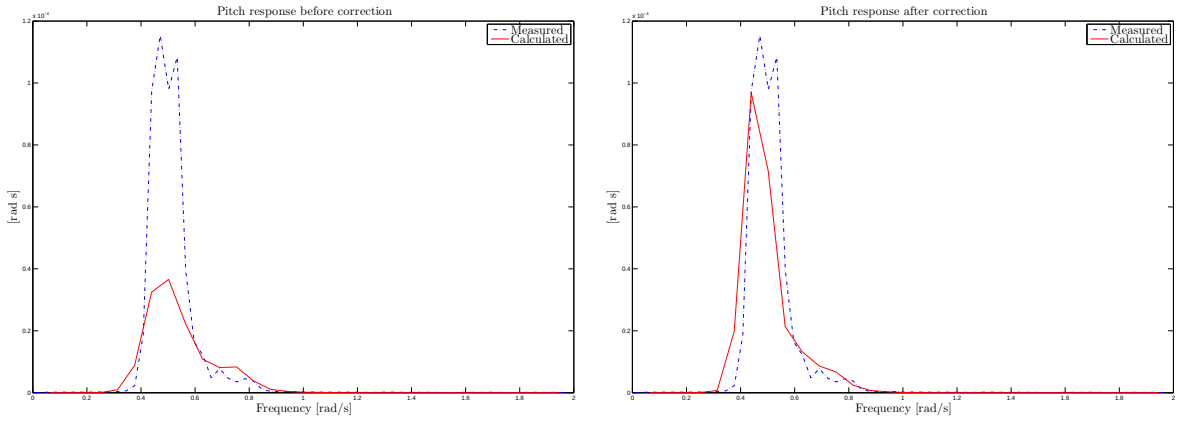

(a) Pitch response before correction

(b) Pitch response after correction

Figure 6.6: Improvement pitch motion prediction visualized after correction with Radac data

In figure 6.6 the result of the data fusion of Wavex data with Radac data is visualized for the pitch motion. As can be seen, using Radac data to correct the amount of each frequency band does improve the heave and pitch response prediction significantly.In figure 6.7 the result of correcting with Radac data is visualized for the complete 14 hours of data.

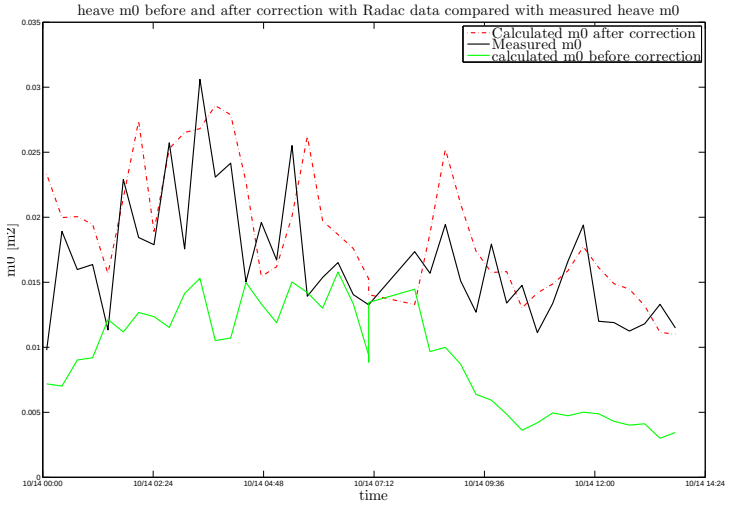

Figure 6.7: Result of Radac correction in heave response domain

6.1.2 Sensitivity analsyis

Since the one dimensional surface elevation measurement by the Radac is used to correct the estimated undisturbed wave spectrum, there is a need to explore its sensitivity to uncertainties. In previous section the relation between the incident wave and the disturbed wave at the measuring location was described. The contributions were divided into two parts. The first relates to the vessel form and the wave approach direction. The second relates to the motion induced waves. Furthermore, as you can imagine, the measure of disturbance has also a strong relation to the location where you measure.
In the initial vessel configuration the vessel has a draft of 9.5 meters and a backwards trim of 0.5 meters. The Radac Waveguide is installed in the middle below the helideck and 6 meters behind the aft perpendicular.

To assess the sensitivity, the sensitivity analysis is divided into three parts. First, the influence of the draft variation will be considered. Change in draft results in a change of the submerged area at the aft of the vessel. As you can imagine, the extent in which the vessel reflect the incoming waves has a strong relation with the surface it reflects to. The change of dynamic behavior of the vessel due to the variation of draft will be dealt with in section 6.2. Second, the transformation of the transom of the vessel depends also on the trim angle of the vessel. In the third part the influence of a small deviation of the measuring location will be considered.

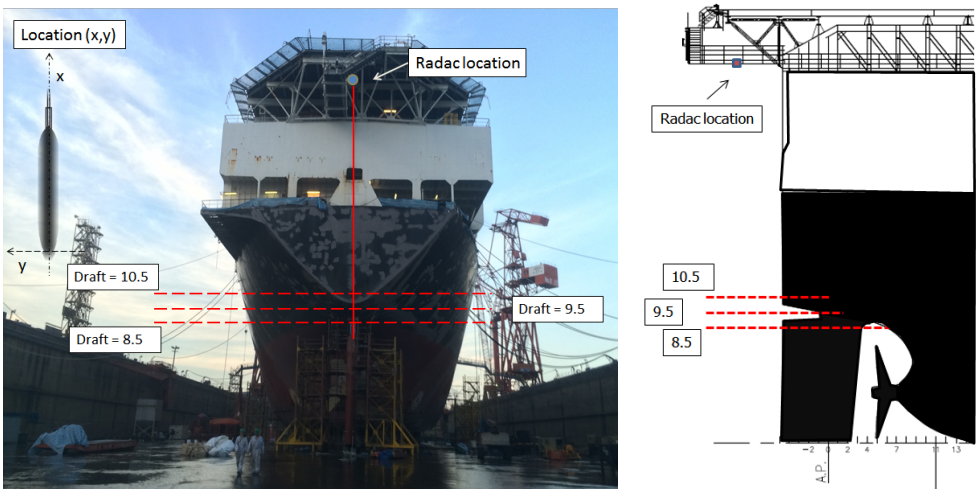

(a) Audacia in dry dock (b) side view

Figure 6.8: Waterline for different drafts

Sensitivity to change of draft

It has to be realized that the change of the fluid point rao due to the variation of draft is determined by multiple effects. In this part only the change of the water playing area at the aft due to the change of draft is considered. The range of variation in the operational drafts is 9.5 ± 1 meter. In figure 6.8a, the waterline at varying draft is depicted. As the draft increases the transom gets more submerged, resulting in a change of the area to which the waves reflect. In figure 6.8b the side view is given to visualize the variation of the transom due to a change of

draft.

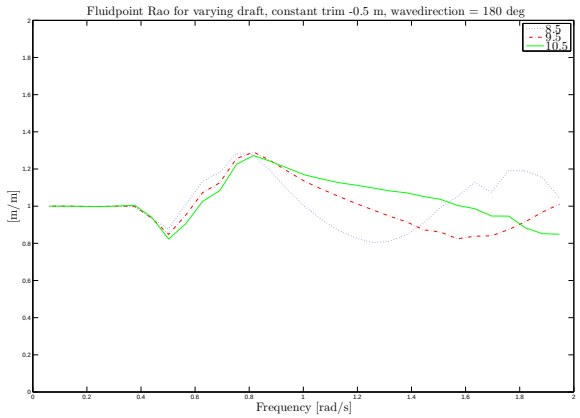

(a) Fluidpoint Rao for stern waves

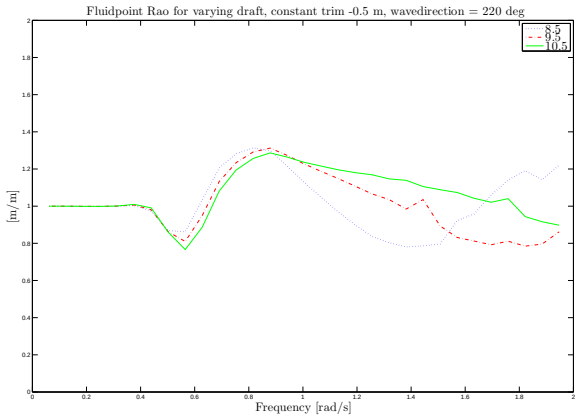

(b) Fluid point Rao for waves coming from 220 degrees.

Figure 6.9: Fluidpoint Raos for stern waves and waves from south-west

In figure 6.9a the fluidpoint raos are plotted for stern waves. It is expected that the diffracted wave potential is affected the most for stern waves as the waves reflect directly on the transom. For sideways waves it is expected that at the draft which the transom is getting submerged the fluid point rao shows an increment of reflected short waves. For head waves the influence due to the change of the draft is expected to be small.

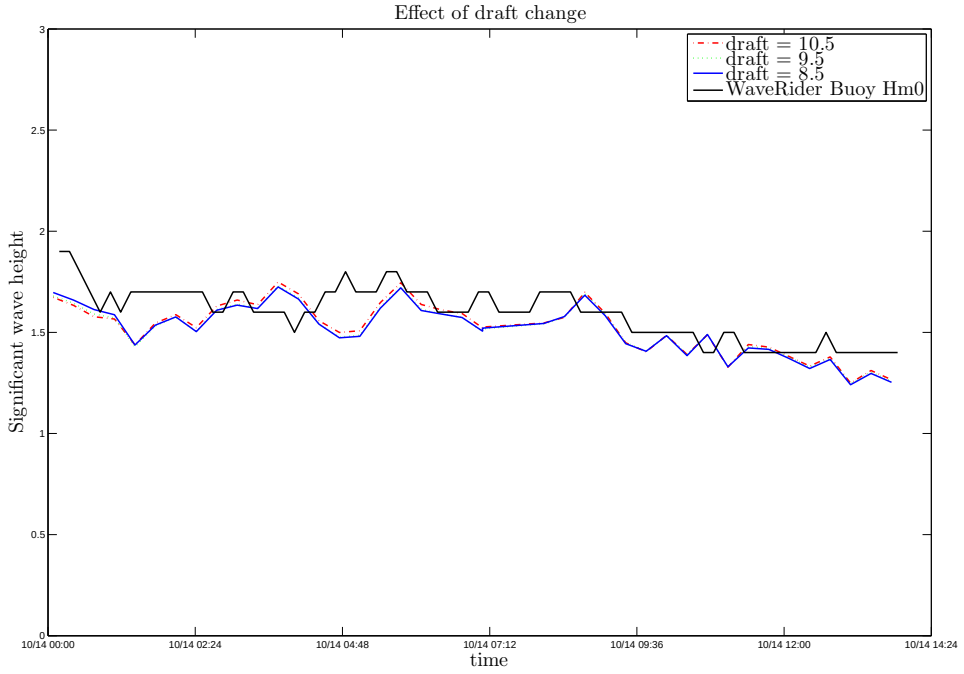

Figure 6.10: Effect of draft change

Sensitivity to trim

Due to relocation of loads on board, the trim angle is not constant. The trim is assumed to be between plus 0.5 meter. In order to assess the influence of the trim on the fluid point rao, the fluidpoint rao is determined for varying trim angles. The draft at lpp/2 is kept constant at 9,5 meters.

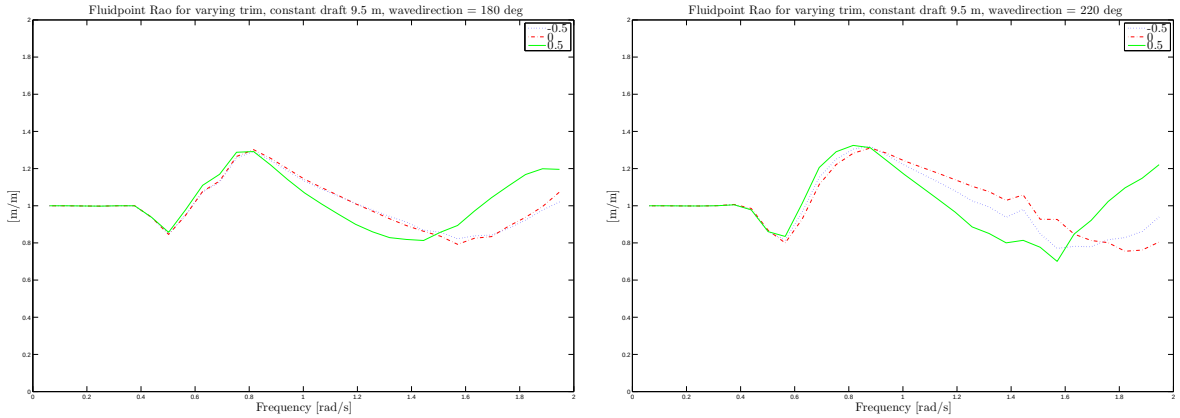

(a) Fluidpoint Rao for stern waves

(b) Fluid point Rao for quartering waves

Figure 6.11: Fluidpoint Raos for stern waves and quartering waves

There is some space between the water surface and the transom when the trim is 0.5 meters forwards. The fluid point raos are therefore be expected to be quite similar for the zero and backward trim as there is in both cases no space between the water surface and the transom. For head waves the influence of the trim is negligible. The influence of the transom getting submerged can be best seen in the fluidpoint raos for waves from starboard.

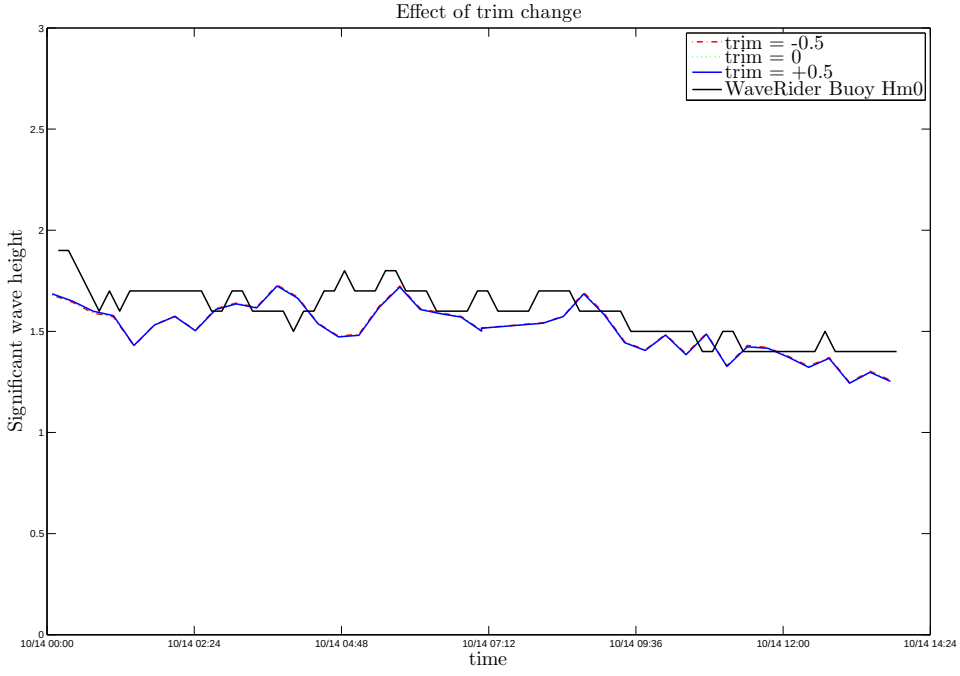

Figure 6.12: Effect of trim change

Sensitivity to Radac measuring location

In this part the influence of a deviation of the measuring location on the fluid point rao is considered.

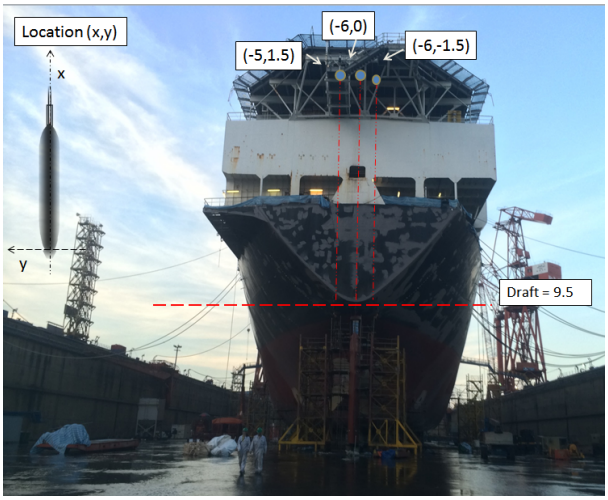

Figure 6.13: Offset in downlooking radar position

The deviation of the location of the installed Radac is assumed to be smaller than 2 meters. In case that the Radac is positioned closer to the transom (smallest distance) the disturbance is expected to be larger. In figure 6.13 the considered Radac location are depicted. The resulting fluidpoint raos for different wave directions are shown in figure 6.14. In figure 6.15 the effect of an offset in the assumed Radac location on the corrected Hs is plotted.

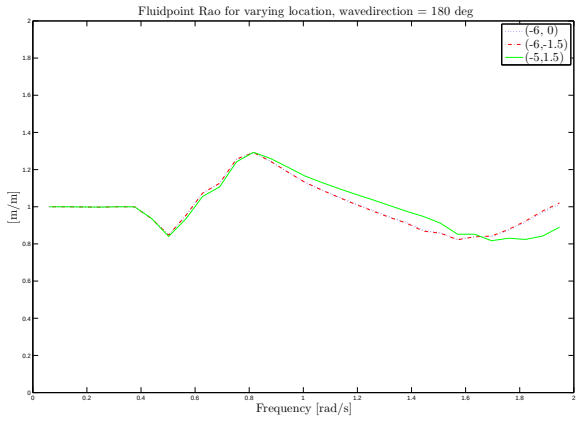

(a) Fluidpoint Rao for stern waves

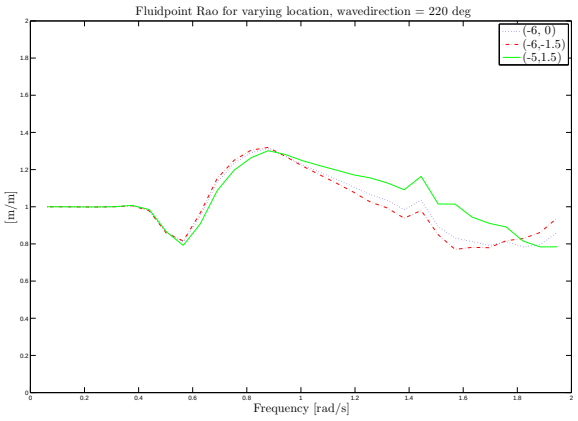

(b) Fluid point Rao for quartering waves

Figure 6.14: Fluidpoint Raos for stern waves and quartering waves

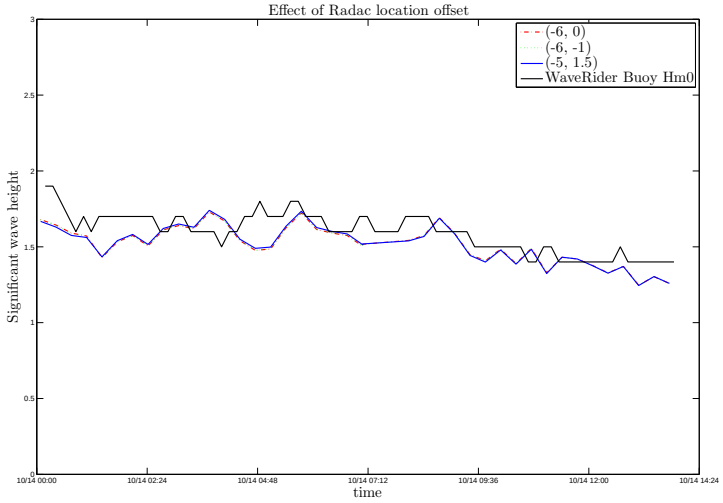

Figure 6.15: Effect of location offset

6.2 Data fusion between Wavex and Octans

In order to investigate whether it is possible to calibrate the amount of energy in the directional wave spectrum estimated by Wavex with measured vessel motions the data have to be comparable. This means that the directional wave spectrum must be converted to motion spectra. In chapter 3 the linear relation between incident waves and vessel response was introduced. The first order vessel response motions can be calculated using the motion raos.
The behaviour of a Audacia in waves is modelled using Aqwa, a engineering suite of tools for the investigation of waves on a fixed or floating structure. In figure 6.16 the first order motion raos are plotted for a few wave directions.

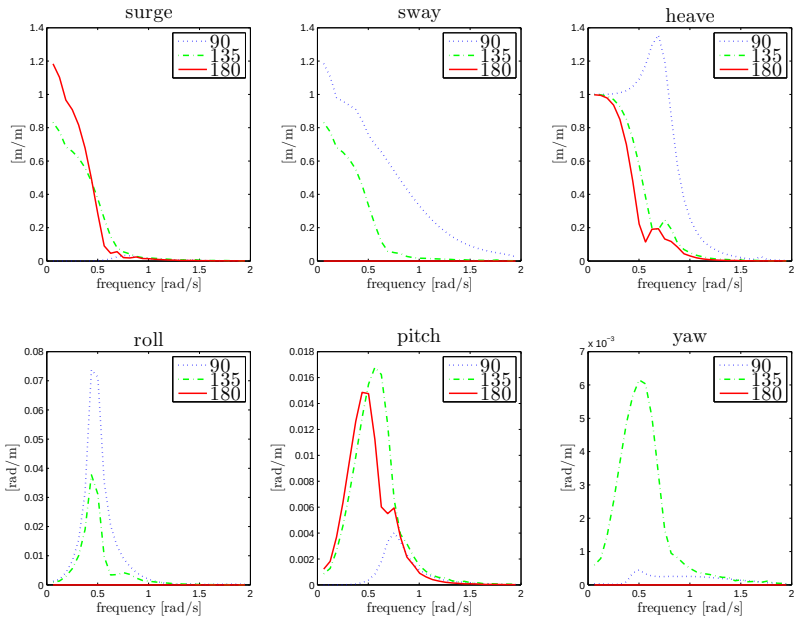

Figure 6.16: Audacia Raos

6.2.1 Sensitivity analsysis

In section 6.1.2 the influence of the variation of draft was explored for the fluidpoint rao. In the fusion of Wavex with the Ixsea, the vessel responses are of great importance. The purpose of this sensitivity analysis is not only to determine the impact of the uncertainties on the motion rao's, but also to determine which vessel motions are suitable to use for the motion data fusion.

To determine the appropriate motions, three effects have to be considered.

- The ship respond to a wave depends on the wave direction. For instance, the vessel does not respond in sway direction for pure stern waves. No surge motion is expected for sideways waves.
- The frequency band width in which the vessel responds to waves.
- The second order effects such as drift forces.

In the following figures the spectra of the measured vessel motions are plotted. In order to illustrate the difference in the amount of energy of the different motions the axes for motions are set equal. For the spectra of the rotations roll and pitch this is also done.

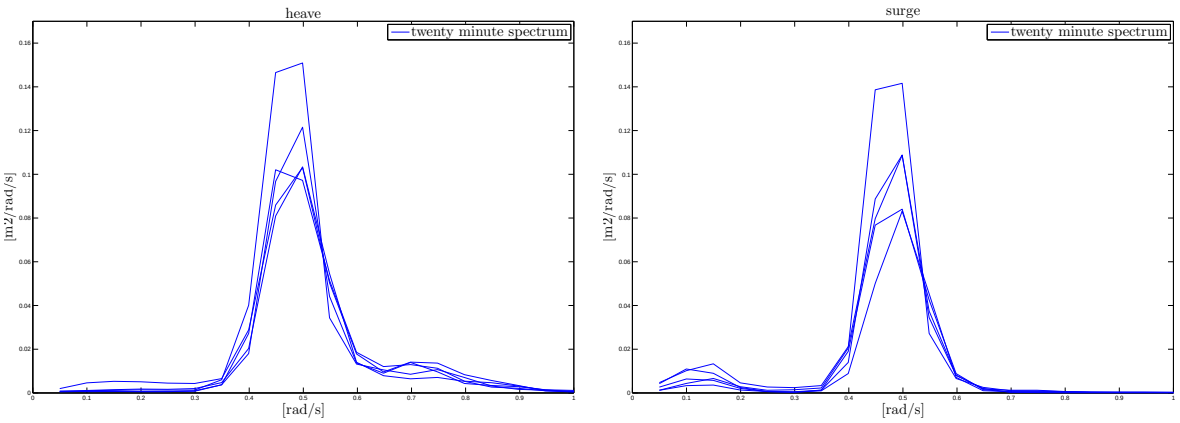

(a) Heave motion response spectra

(b) Surge motion response spectra

Figure 6.17: Response spectra for multiple time periods

In chapter 5 it was shown that the sea state was dominated by stern waves. As these were real time measurements, the influence of the dominant wave directions should be visible in the response spectra. The amount of energy in the roll and sway motion is small in comparison with the heave, pitch and surge motion. As it can be seen, the measured surge motion is also affected by the wave induced second order drift forces.
In figure 6.18a the amount of energy in the heave motion is compared with the amount of energy in the sway motion 6.18b. Since the the wave field is dominated by stern waves, the sway response is as expected low. It must be realised that for beam waves the second order drift forces would be visible in the sway response spectra.
For stern waves, no roll motion are expected. In case of beam waves, roll motion could be expected. However, roll motions are difficult to calculate correctly due to the sensitivity to load variations and has a non-linear and resonant behaviour [12]. Hence, the measured heave and pitch motion will be used to correct the amount of energy in the estimated wavex wave spectrum.

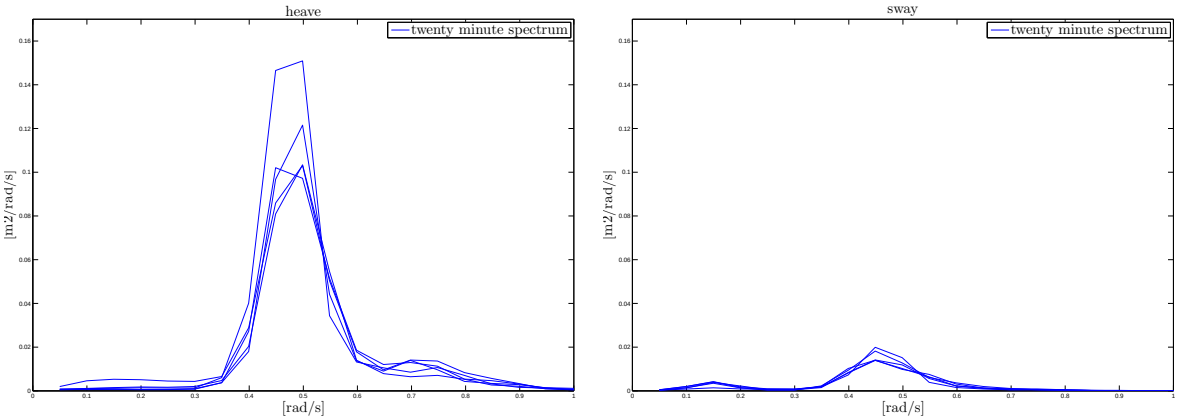

(a) Heave motion response spectra

(b) Sway response motion spectra

Figure 6.18: Response spectra for multiple time periods

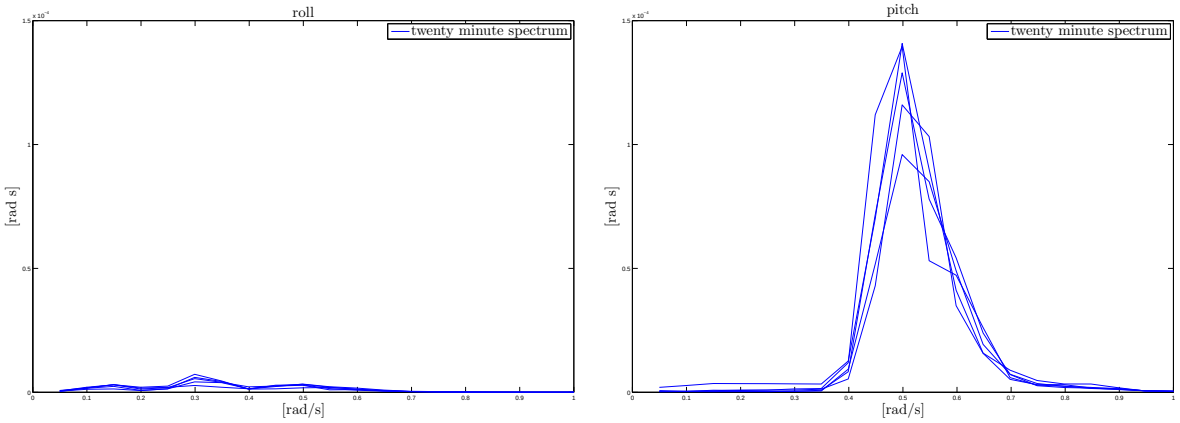

(a) Roll motion response spectra

(b) Pitch motion response spectra

Figure 6.19: Response spectra for multiple time periods

Sensitivity to change of draft

Since the draft vary during offshore operations, the sensitivity of the ship response to a change of draft is explored. A change of draft results in change of the inertia. As the ship respond depends on the inertia, the change of draft may affect the dynamic behaviour.
The moments of inertia are often expressed in terms of the radii of inertia and mass of the vessel (the water displacement multiplied with the water density). In order to asses how the draft affects the motion Raos, the relation between the water displacement and its of moments of inertia are kept constant by keeping the radii of inertia constant.

$$I_{xx} = k_{xx}^2 \cdot \rho\nabla \tag{6.1}$$

$$I_{yy} = k_{yy}^2 \cdot \rho\nabla \tag{6.2}$$

$$I_{zz} = k_{zz}^2 \cdot \rho\nabla \tag{6.3}$$

with k_{ii} the radii of inertia known, the inertia moments can be calculated. Since the software packet does not taken into account viscous effects, roll damping has to be added to avoid

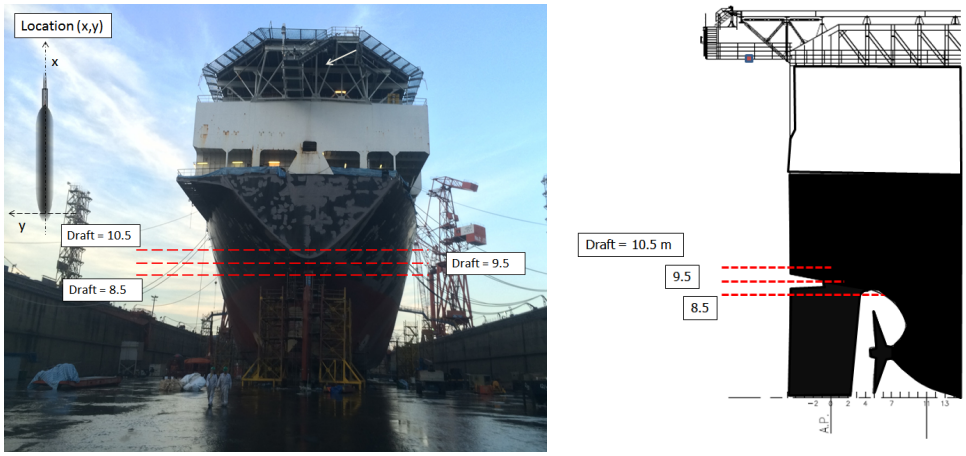

(a) Audacia in dry dock (b) side view

Figure 6.20: Waterline for different drafts

unrealistic roll motions. The roll damping is calculated with the following relation.

$$B_{\phi\phi} = 2 \cdot \kappa \cdot \sqrt{C_{\phi\phi} \cdot (I_{\phi\phi} + I_{\phi\phi ADD})} \tag{6.4}$$

with: $C_{\phi\phi}$ is the roll stiffness, $I_{\phi\phi}$ is the roll inertia and $I_{\phi\phi ADD}$ is the extra roll inertia due to added mass. Based on experiences of Allseas a κ value of 0.1 is used.

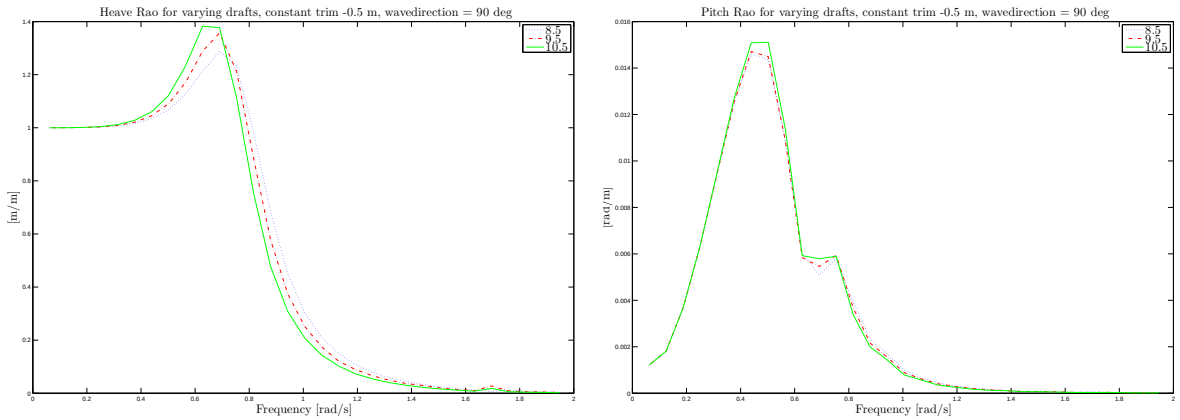

(a) Heave Rao (b) Pitch Rao

Figure 6.21: Effect of varying draft on motion raos for beam waves

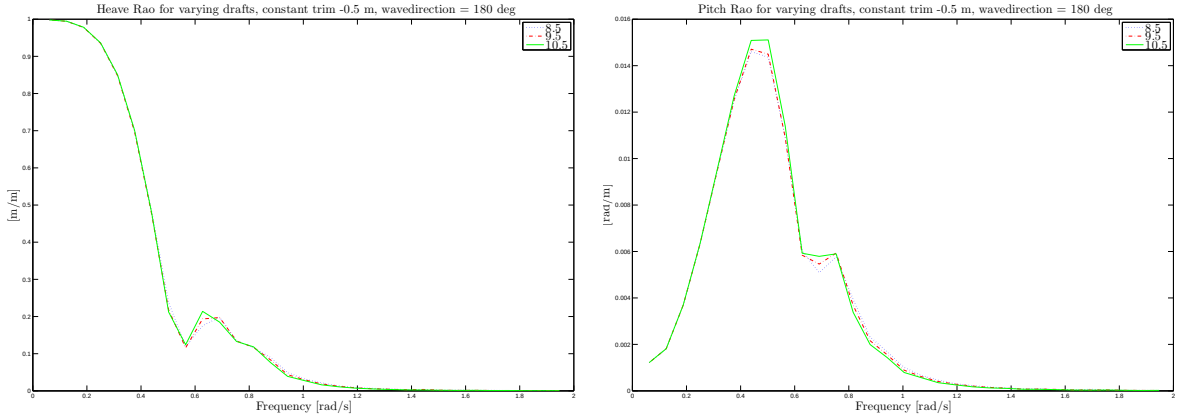

(a) Heave Rao (b) Pitch Rao

Figure 6.22: Effect of varying draft on motion raos for stern waves

Sensitivity to change of trim

To determine the influence of the trim angle of the ship, the influence of the trim on the raos is explored. The draft at $l_{pp}/2$ is kept constant. As the ship is not symmetric in lateral direction, the change in water displacement has to be taken into account.

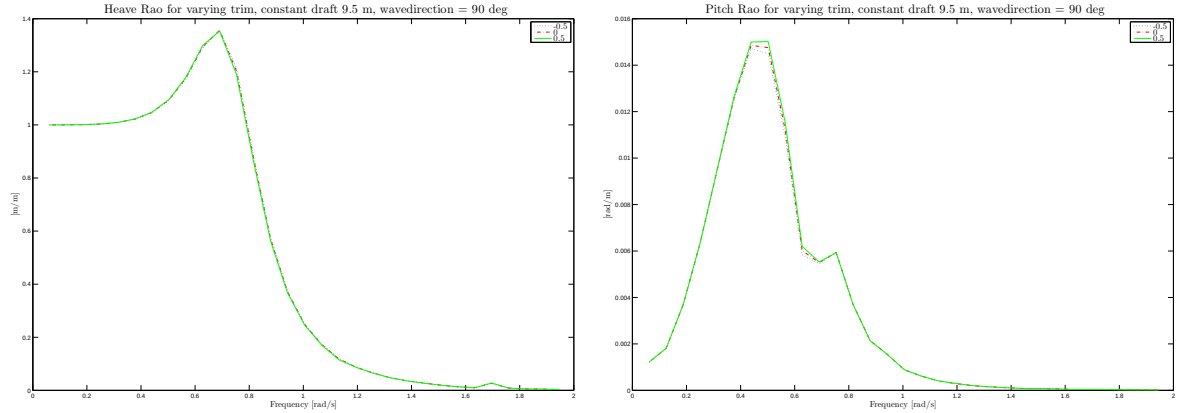

(a) Heave Rao (b) Pitch Rao

Figure 6.23: Effect of varying trim on motion raos for beam waves

6.2.2 Correction

The equation for the frequency dependent scaling factor based on vessel motion, introduced in chapter 5, is now limited to the heave motion and pitch rotation and can be written as:

$$r(\omega) = \int_{\omega-\Delta\omega}^{\omega+\Delta\omega} \frac{\phi_{3,m}(\omega) + \phi_{5,m}(\omega)}{\phi_{3,p}(\omega) + \phi_{5,p}(\omega)} \, d\omega \tag{6.5}$$

with:

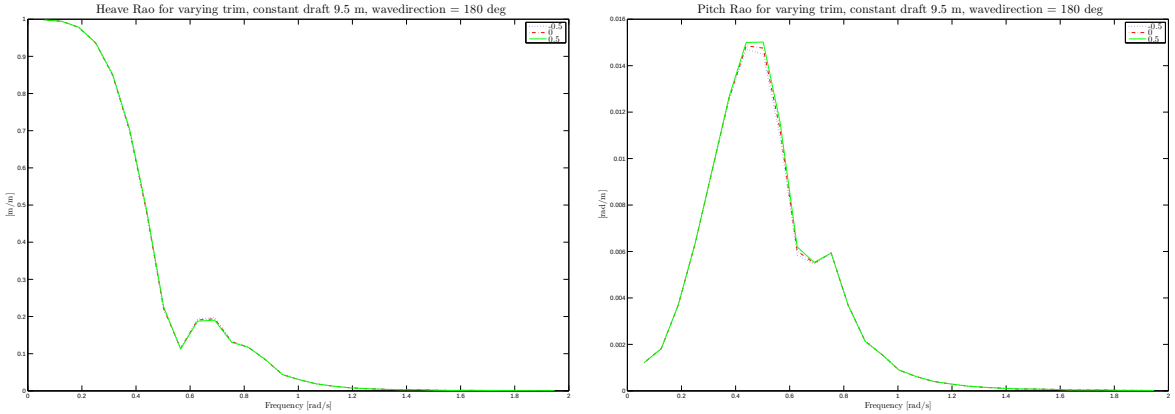

(a) Heave Rao

(b) Pitch Rao

Figure 6.24: Effect of varying trim on motion raos for stern waves

$\phi_3(\omega)$	Heave motion spectrum
$\phi_3(\omega)$	Pitch motion spectrum
m	Spectra measured by motion sensors
p	Predicted based on Wavex directional wave frequency spectrum

The frequency dependent ratio is used to correct the amount of energy at each frequency in the directional wave spectrum given by the Wavex.

Define correction cut-off frequency

The main thesis objective is to improve the amount of energy in the directional wave spectrum, this means that satisfying the conditions that the measured responses match the calculated responses is not the priority. The energy in the wave is proportional to the square of the wave height. Said that, not the relative importance of both motions, but the vertical motion due is considered. The second effect what has to be taken into account is the frequency band width in which the vessel respond to waves. Firstly, regarding to very short waves with respect to the ship's length, the ship does not respond to such excitations. For waves with a very long wavelength with respect to the ship's length it will almost only respond by following the surface elevation in a pure heave motion. Secondly, as the pitch motion does not have a direct relation to the surface elevation, the vertical motion at the bow due to pitch is used to determine the relative importance. As the frequency band width in which the vessel respond to waves depend on the wave direction, the frequency band width for which the Wavex can be corrected is also dependent on the wave direction.

$$r(\omega) = \int_{\omega-\Delta\omega}^{\omega+\Delta\omega} \frac{a \cdot \phi_{3,m}(\omega) + b \cdot \phi_{5,m}(\omega)}{a \cdot \phi_{3,p}(\omega) + b \cdot \phi_{5,p}(\omega)} \, d\omega \tag{6.6}$$

In which a and b are normalised values which stand for the relative importance of the motion. The cut-off frequency is chosen to be at the frequency that the heave rao become smaller than 0.05. For wave frequencies higher than the cut-off frequency the spectrum is not corrected. The lowest correction is for stern waves. The cut-off frequency for stern waves is $1\,rad/s$.

6.2.3 Results

In this section the results of using vessel motions to improve the wave spectrum estimation are discussed. The corrected wave spectrum Hs is compared to the Hs measured by the WaveRider wave buoy. Second, the surge and sway motion response spectra are calculated using the corrected wave spectrum as input. These calculated motion spectra are compared with the measured vessel motion spectra.

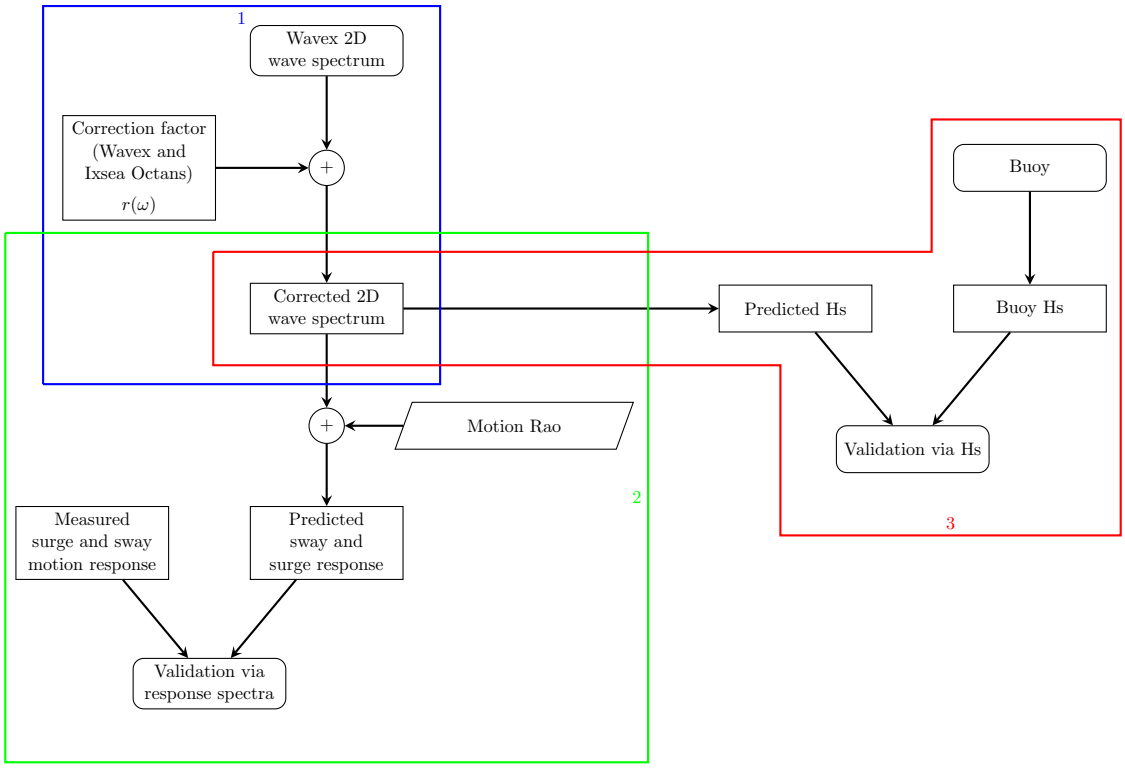

Figure 6.25: Flowchart using vessel motion validation

Comparison with WaveRider wave buoy

In figure 6.26 the result is plotted for the 14 hours of data. The correlation between the corrected Wavex Hs and the Hs measured by the buoy is weaker than using Radac WaveGuide measurements to correct the Wavex wave height. It must be realised that the Hs is calculated using:

$$Hs = 4 \cdot \sqrt{\int_0^\infty S(\omega)\, d\omega} \tag{6.7}$$

So the Hs is based on the amount of energy in the entire wave spectrum. As mentioned before, the amount of energy is not corrected for frequencies higher than the cut-off frequency. Therefore the Hs is also affected by the amount of energy in the uncorrected wave frequencies.

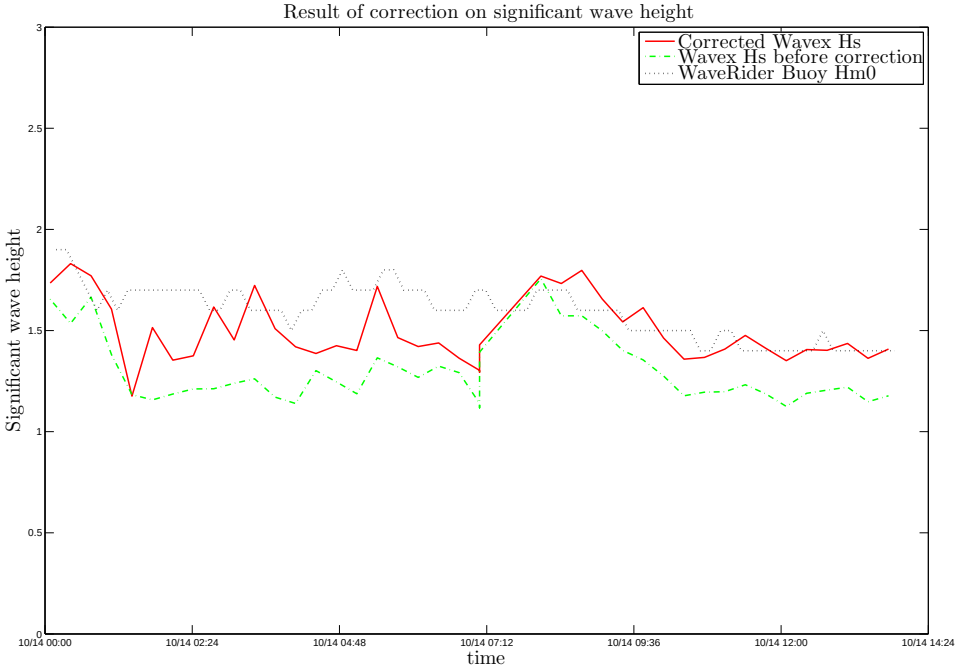

Figure 6.26: Result of Wavex Correction

Comparison with measured vessel motion response spectra

Vessel motions were used to correct the amount of energy in each frequency band by using multiple motions. In figure 6.27 the achieved improvement is shown for the heave and pitch motion.

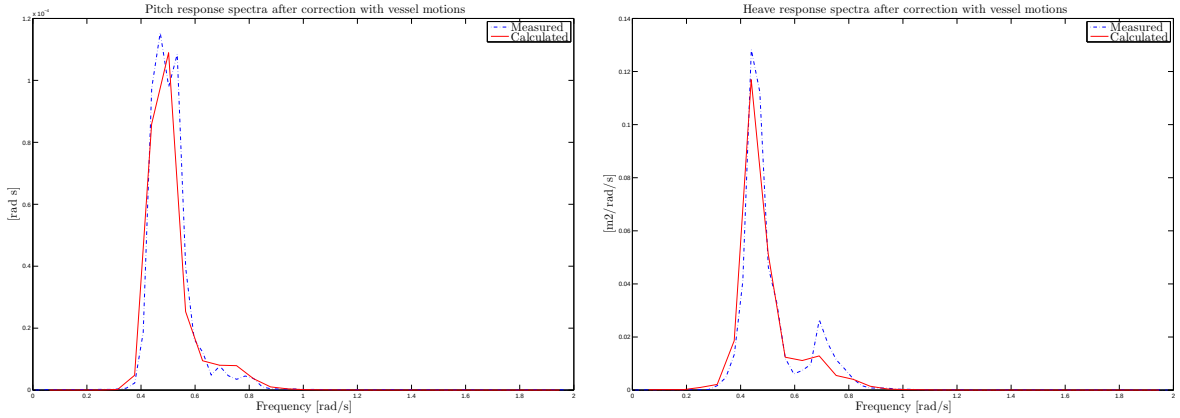

(a) Pitch response spectra after correction

(b) Heave motion spectra after correction

Figure 6.27: Improvement heave and pitch motion prediction visualized after correction with vessel motion data

But since the heave and pitch motion were used to correct the directional wave spectrum, it is obvious that those motions could be predicted more correctly after applying the data fusion. Therefore, in order to validate the improvement the motions that were not used to determine the correction factor are plotted as well. In figure 6.28 the surge motion comparison is plotted. The second order surge effects were also measured by the motion sensors. However, the

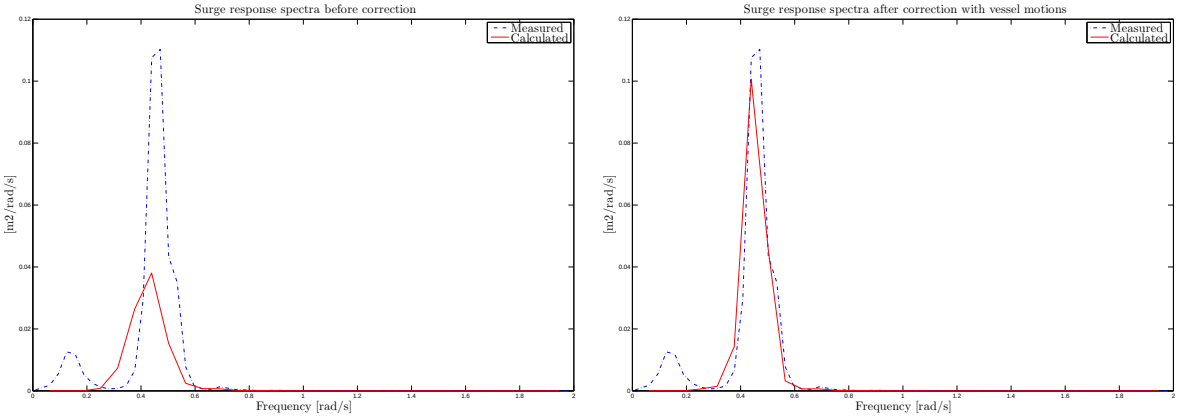

(a) Surge motion spectra before correction

(b) Surge motion spectra after correction

Figure 6.28: Improvement first order surge motion prediction visualized after correction with vessel motion data

second order effects are not calculated based on the directional wave spectrum. The calculated first order surge motion has a strong correlation to the measured surge motion after correction.

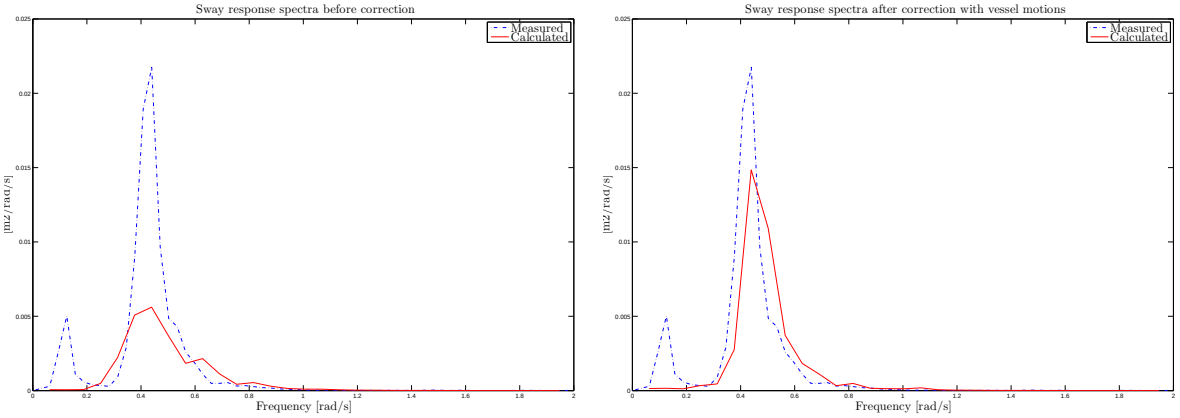

(a) Sway motion spectra before correction

(b) Sway motion spectra after correction

Figure 6.29: Improvement first order sway motion prediction visualized after correction with vessel motion data

To visualize the improvement for the whole measuring period, the zero order moment is calculated for the surge motion. In green the zero-order moment calculated based on the Wavex wave spectrum. In red the zero-order moment after correcting the directional wave spectrum using vessel motions.

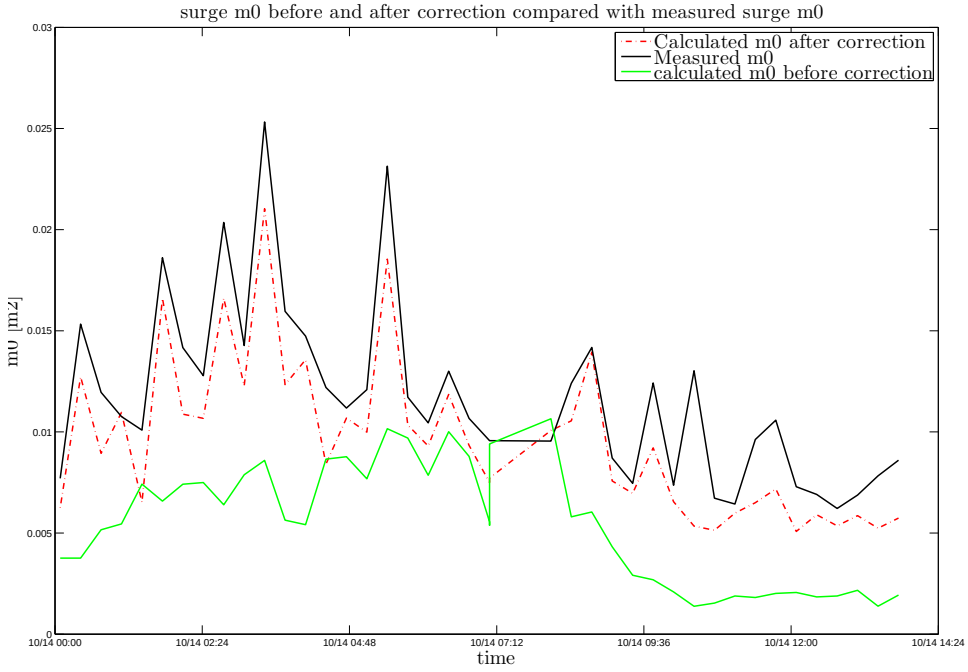

Figure 6.30: Result of correction in surge response domain

Chapter 7

Conclusion and recommendations

The objective of the study was to improve the current Wavex wave spectrum without using any instruments deployed in the water. It is investigated whether combining the data measured by one or the other device to the X-band radar data result in an improvement of the radar estimated directional wave spectrum, and which combination gives the best results.

Method

In order to improve the directional wave spectrum estimations (2D wave spectrum) given by the X-Band radar used on board of the Audacia (Wavex from Miros), the possibility of using an extra measuring instrument to calibrate the energy is investigated. Two measuring devices are considered.

- A down looking radar, recently installed below the helideck of the Audacia, measuring the single point surface elevation (1D wave spectrum) in vicinity of the vessel. (Radac WaveGuide)
- The MRU sensors, which measure the wave induced vessel motions (Ixsea Octans).

Conclusions

It is possible to improve the wave spectrum estimation on board with an extra measuring instrument.

Wavex and Radac data fusion. The Hs has a strong correlation to the Hs measured by the wave buoy in vicinity of the vessel after correcting the wave spectrum with a frequency dependent scaling factor. Before correcting the Hs has an average deviation of 30 centimetres, after correction the Hs deviation is reduced to 10 centimetres. The vessel response spectra calculated using the linear relation between incident waves and vessel response has strongly improved after correcting the amount of energy in each frequency with the Radac measurement.

Wavex and Octans data fusion The Hs after correction with a frequency dependent scaling factor determined by using the heave and pitch motion has a strong correlation to the Hs measured by the WaveRider wave buoy. However, the Hs fluctuates more from the Hs measured by the buoy than the Hs determined by using Wavex and Radac data fusion. The average deviation however is also within the 15 centimetre range. Comparing the calculated vessel motion after correcting, the Wavex and Octans data fusion gives a better result, see figure 7.1.

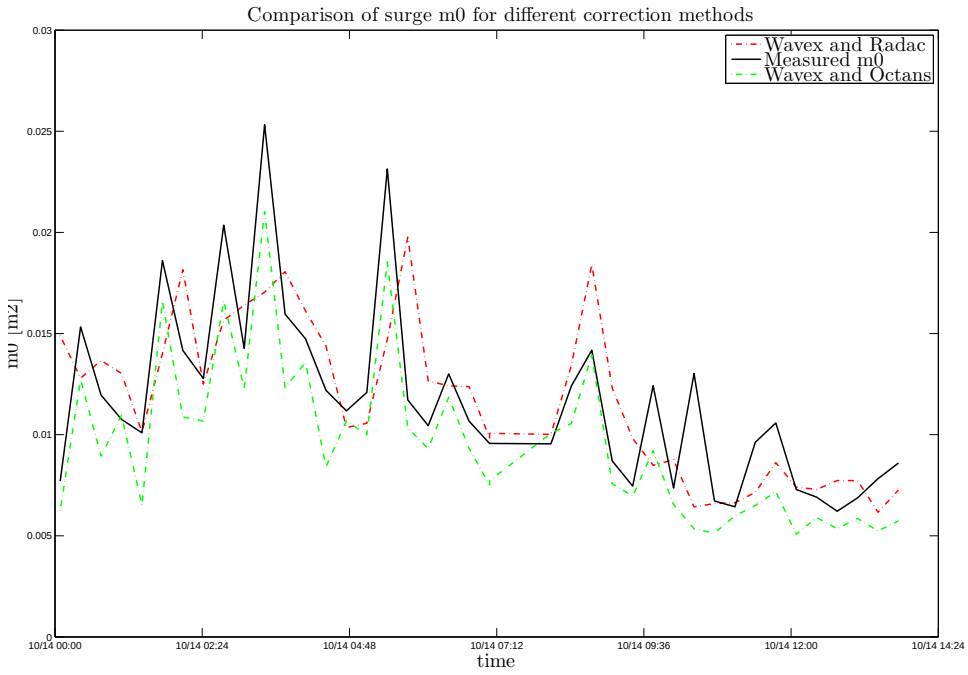

Figure 7.1: Result of correction in surge response domain

Recommendations

- It has to be investigated whether it is possible to combine the Wavex wave spectrum with the Radac measurements and the vessel motion measurements.
- The sea state during the case study was dominated by stern waves. It has to be investigated if it is also possible to use this method for different wave directions. (For stern waves the measuring location is not that much disturbed by shielding effects). The method is tested for 14 hours of measurements only; it must be tested for longer period and for different wave conditions.
- Using the analysing principle of the Wavex there is no unique relation between the radar backscatter and the Hs. However, Dankert claims that he has developed a method which does not need calibration. It should be investigated whether it is possible to determine a directional wave spectrum in agreement with the wave buoy using his method.
- The methods are tested for the Audacia, it has to be investigated whether this method can be applied for a random vessel.

Bibliography

[1] Nieto Borge. *Use of nautical radar as a wave monitoring instrument.* Coastal Engineering 37, page 331342, 2003.

[2] H. Dankert. *Measurement of Waves, Wave Groups and Wind Fields using Nautical Radar-Image Sequences.* GKSS, 2004.

[3] H. Dankert and W. Rosenthal. *Ocean surface determination from X-band radar-image sequences.* Journal of geophysical research, Vol. 109, 2004.

[4] A. Van der Vlught. *Quotation, WaveGuide on Board.* 2013.

[5] Toshio Iseki. *Bayesian estimation of directional wave spectra based on ship motions.* Control Engineering Practice 8, page 215 - 219, 2000.

[6] J.M.J Journe and W.M. Masie. *Offshore hydromechanics.* Delft University of Technology, 2001.

[7] U.D Nielsen. *Estimation of directional wave spectra from measured ship responses.* Technical University of Denmark, 2005.

[8] U.D Nielsen. *Estimations of on-site directional wave spectra from measured ship responses.* Marine Structures 19, page 3369, 2006.

[9] U.D. Nielsen and David C. Stredulinsky. *Sea state estimation from an advancing ship A comparative study using sea trial data.* Applied Ocean Research, volume 34, page 33-44, 2012.

[10] Rafael Sandrea and Ivan Sandrea. *Deepwater crude oil output: How large will the uptick be?* Oil and Gas Journal, 11.

[11] David C. Stredulinsky and E.M. Thornhill. *Ship Motion and Wave Radar Data Fusion for Shipboard Wave Measurement.* Journal of ship research vol 55, No. 2, page 73-85, 2011.

[12] E.A Tannuri and J.V. Sparano. *Estimating directional wave spectrum based on stationary ship motion measurements.* Applied Ocean Research, volume 25, page 243-261, 2003.

Chapter 8

Appendix

8.1 Sensitivity Fluidpoint Rao to trim

The sensitivity of the fluid point rao to trim for head waves and beam waves. For head waves, the influence of trim is negligible. For beam waves the submerged are at the aft increases for backwards trim, the hight frequency waves in the wave spectrum are affected due to the change of water playing area at the aft.

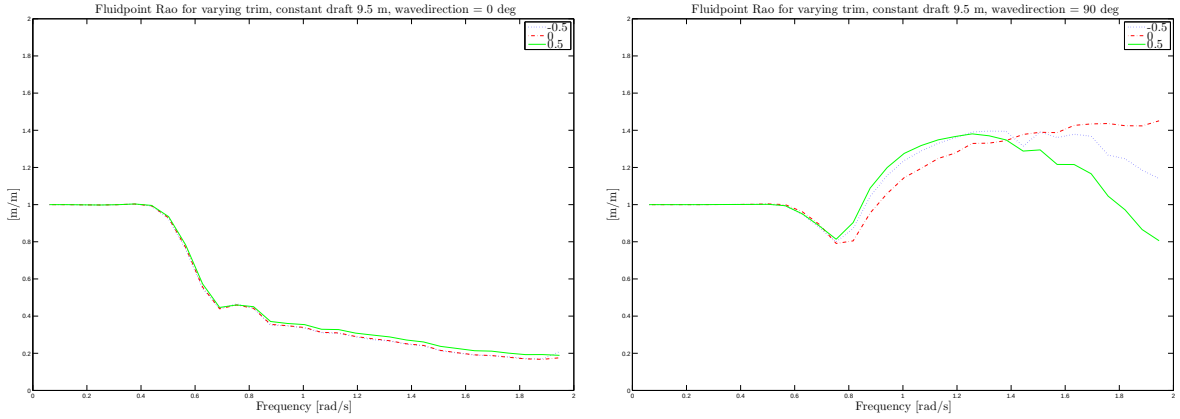

(a) Fluidpoint Rao for head waves

(b) Fluid point Rao for beam waves

Figure 8.1: Fluidpoint Raos for head waves and beam waves

8.2 Sensitivity Fluidpoint Rao to draft

As the sea state during the test case was dominated by following waves, the plots for the sensitivity of the fluid point rao for head waves and beam waves is shown here. For beam waves the influence of the change of draft is visible for the high frequency waves. The water playing area is changed significant when the transom is getting submerged.

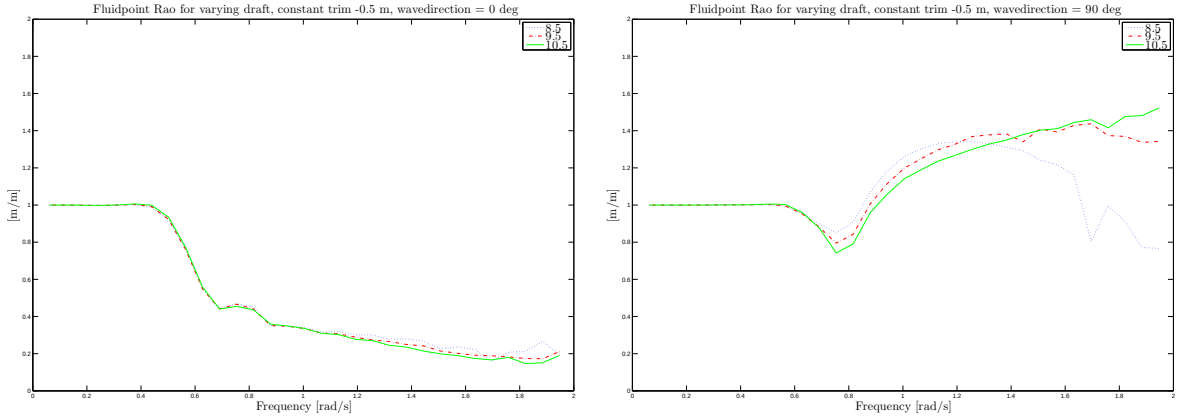

(a) Fluidpoint Rao for head waves

(b) Fluid point Rao for beam waves

Figure 8.2: Fluidpoint Raos for head waves and beam waves

8.3 Sensitivity to Fluidpoint Rao location

For head waves the same in dependency is seen. For beam waves, the closer the Radac is positioned to the transom, the more the high frequency waves are amplified.

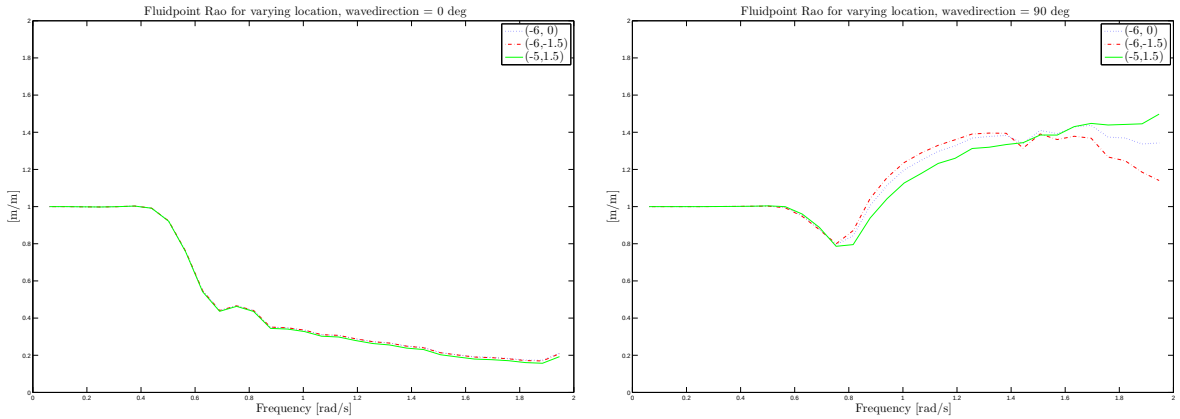

(a) Fluidpoint Rao for head waves

(b) Fluid point Rao for beam waves

Figure 8.3: Fluidpoint Raos for head waves and beam waves

8.4 Sensitivity Motion Rao to draft change

The heave and pitch motion data was used in combination with the Wavex data to determine a directional wave spectrum. In chapter 5 the sensitivity was checked for the dominant wave direction. In response amplitude operators of the heave and pitch motion are plotted here for different approach directions.

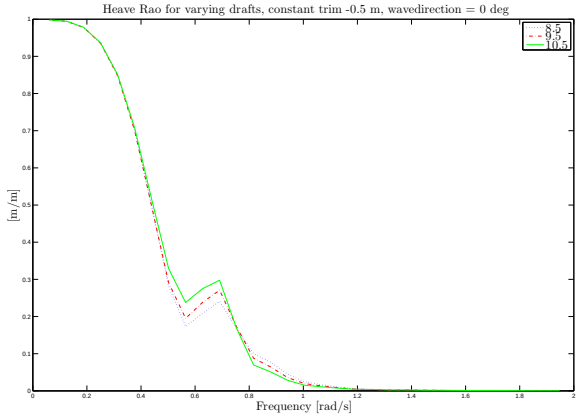

(a) Heave Rao

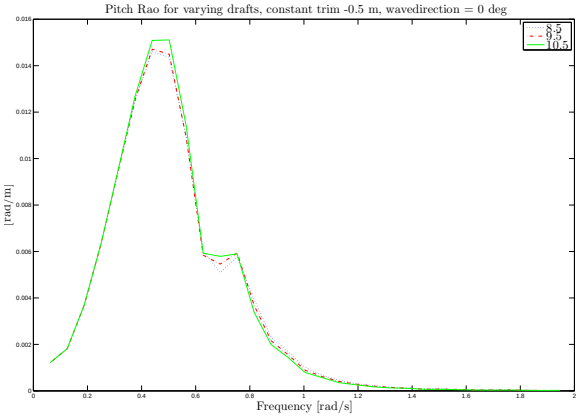

(b) Pitch Rao

Figure 8.4: Effect of varying draft on motion raos for head waves

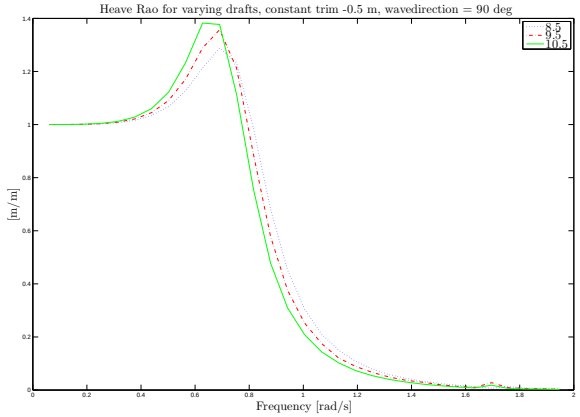

(a) Heave Rao

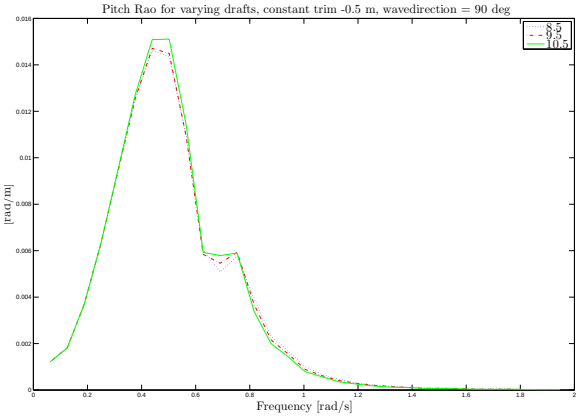

(b) Pitch Rao

Figure 8.5: Effect of varying draft on motion raos for beam waves

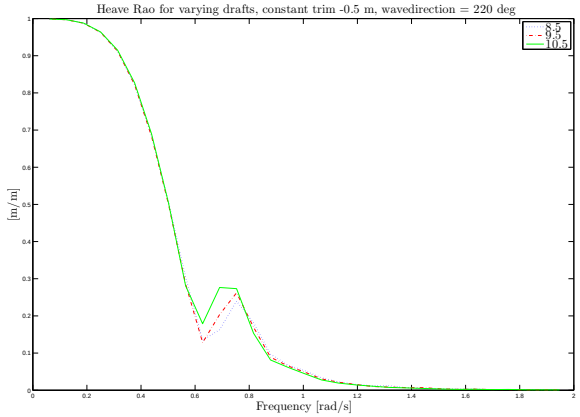

(a) Heave Rao

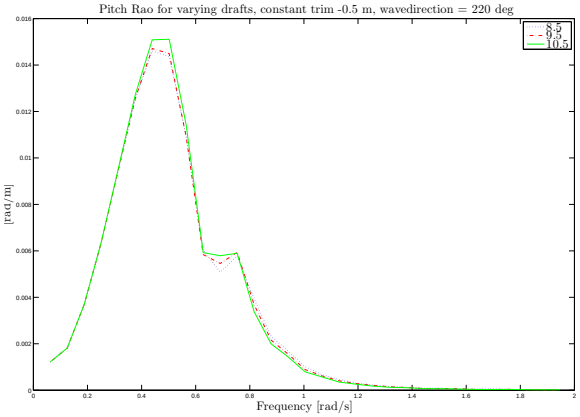

(b) Pitch Rao

Figure 8.6: Effect of varying draft on motion raos for quartering waves

8.5 Results radac data fusion in response domain

In this section the results of the data fusion of Radac data and Wavex data is plotted in the frequency response domain. In the case study the wave spectrum was corrected for 14 hours. The data was cut in periods of 20 minutes for spectral analysis reasons. The time period is depicted in the figure title.

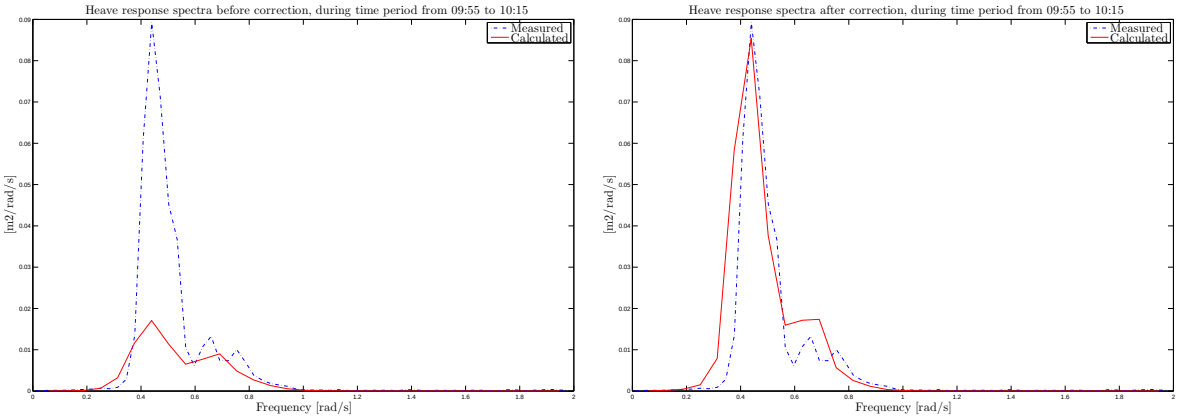

(a) Heave Resonse spectra before correction (b) Heave Resonse spectra after correction

Figure 8.7: Correction visualized in response domain

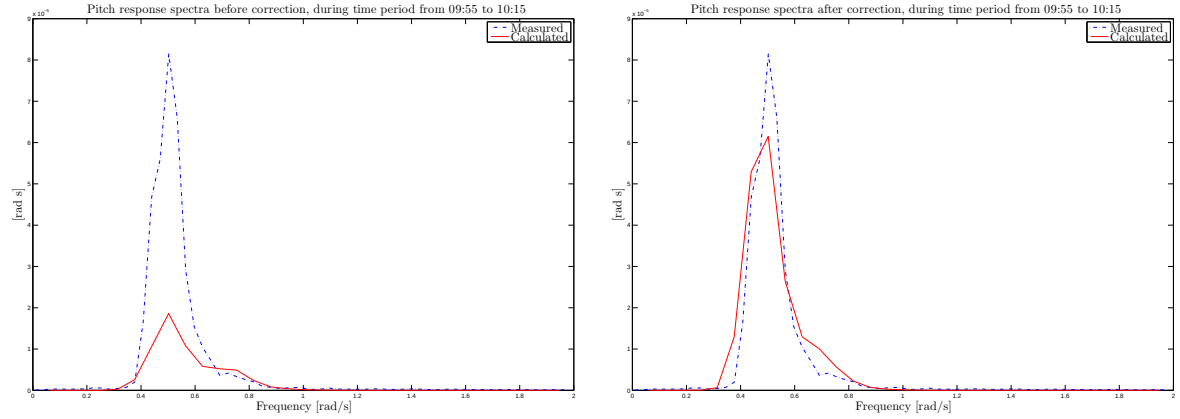

(a) Pitch Resonse spectra before correction (b) Pitch Resonse spectra after correction

Figure 8.8: Correction visualized in response domain

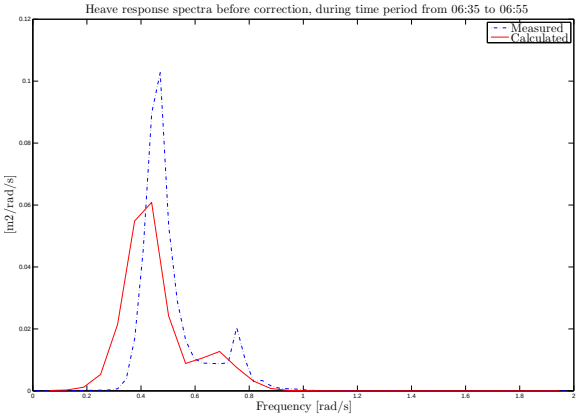

(a) Heave Resonse spectra before correction

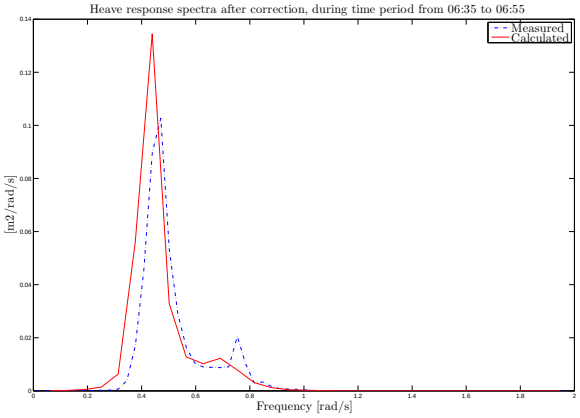

(b) Heave Resonse spectra after correction

Figure 8.9: Correction visualized in response domain

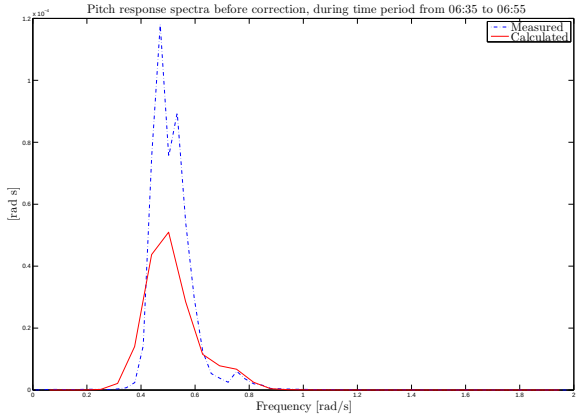

(a) Pitch Resonse spectra before correction

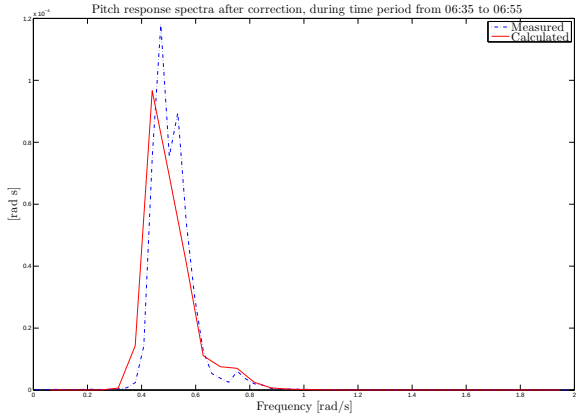

(b) Pitch Resonse spectra after correction

Figure 8.10: Correction visualized in response domain

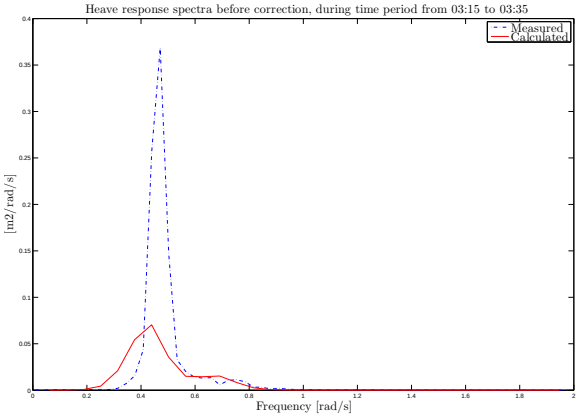

(a) Heave Resonse spectra before correction

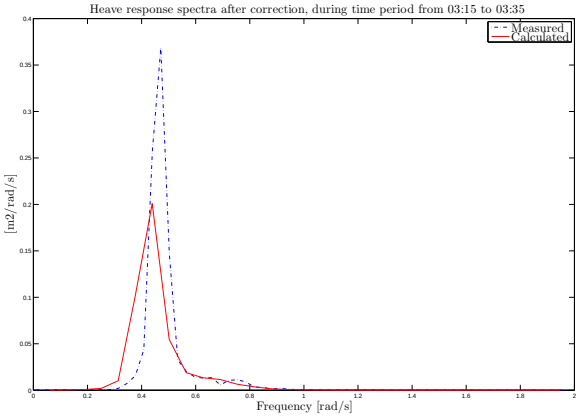

(b) Heave Resonse spectra after correction

Figure 8.11: Correction visualized in response domain

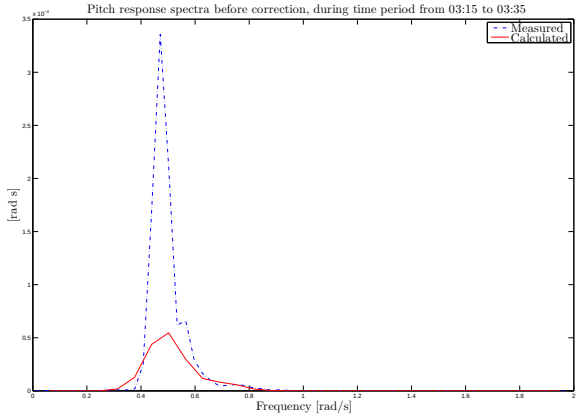

(a) Pitch Resonse spectra before correction

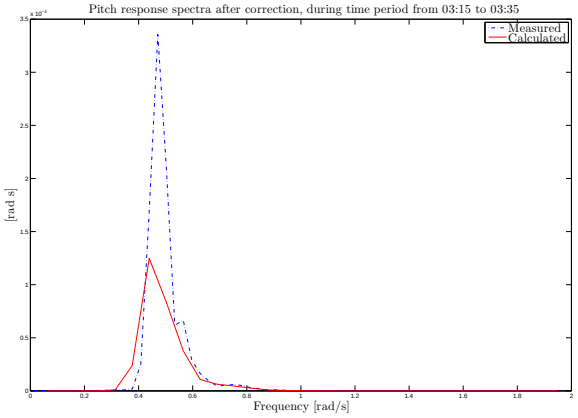

(b) Pitch Resonse spectra after correction

Figure 8.12: Correction visualized in response domain

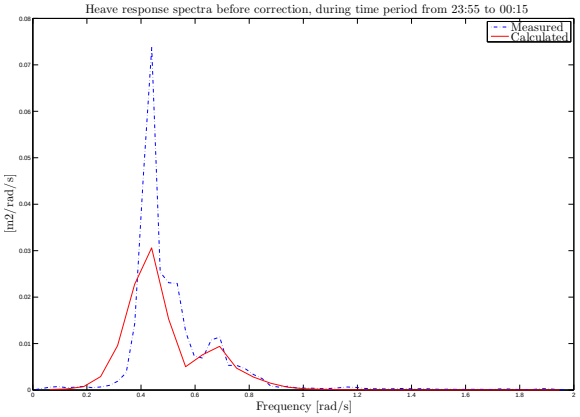

(a) Heave Resonse spectra before correction

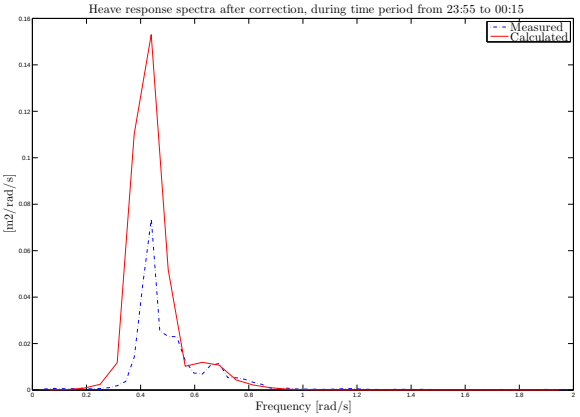

(b) Heave Resonse spectra after correction

Figure 8.13: Correction visualized in response domain

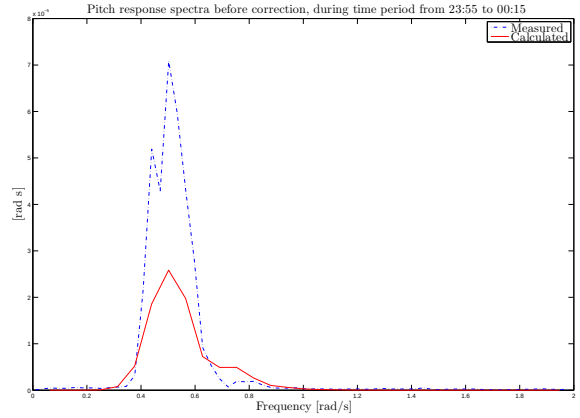

(a) Pitch Resonse spectra before correction

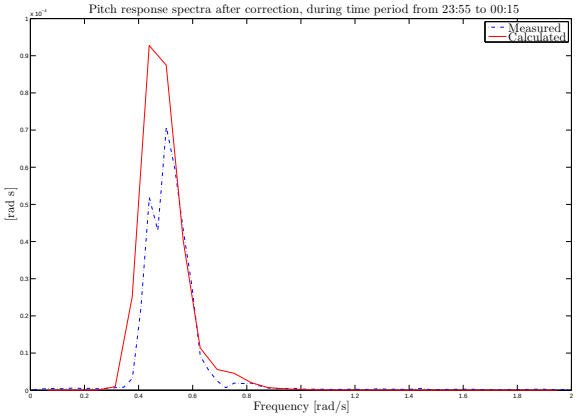

(b) Pitch Resonse spectra after correction

Figure 8.14: Correction visualized in response domain

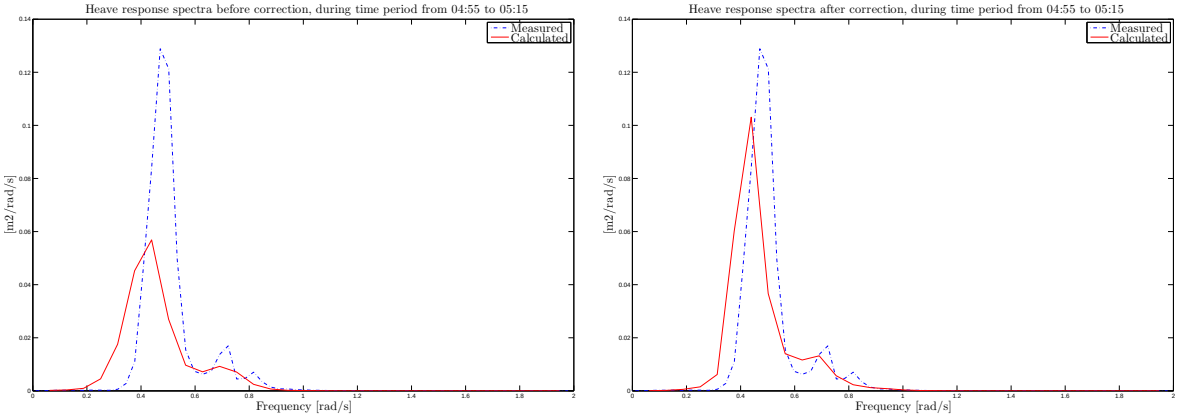

(a) Heave Resonse spectra before correction (b) Heave Resonse spectra after correction

Figure 8.15: Correction visualized in response domain

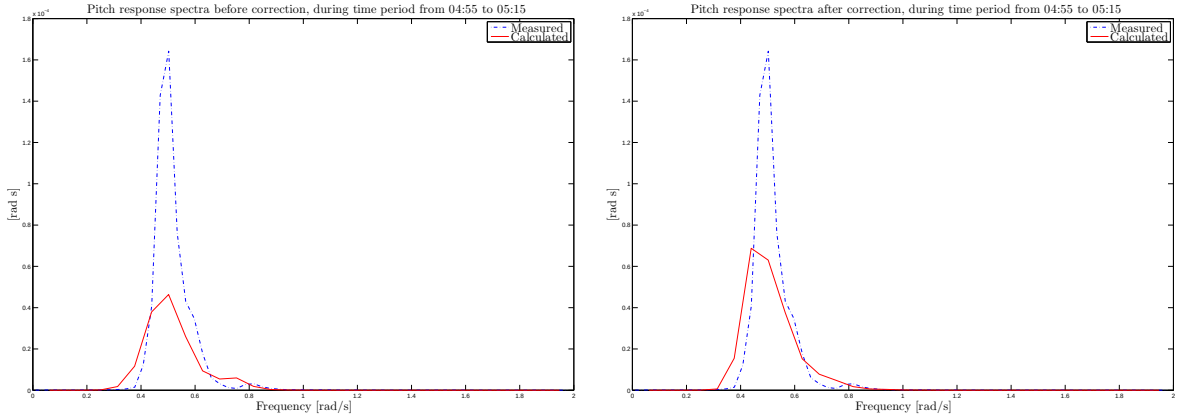

(a) Pitch Resonse spectra before correction (b) Pitch Resonse spectra after correction

Figure 8.16: Correction visualized in response domain